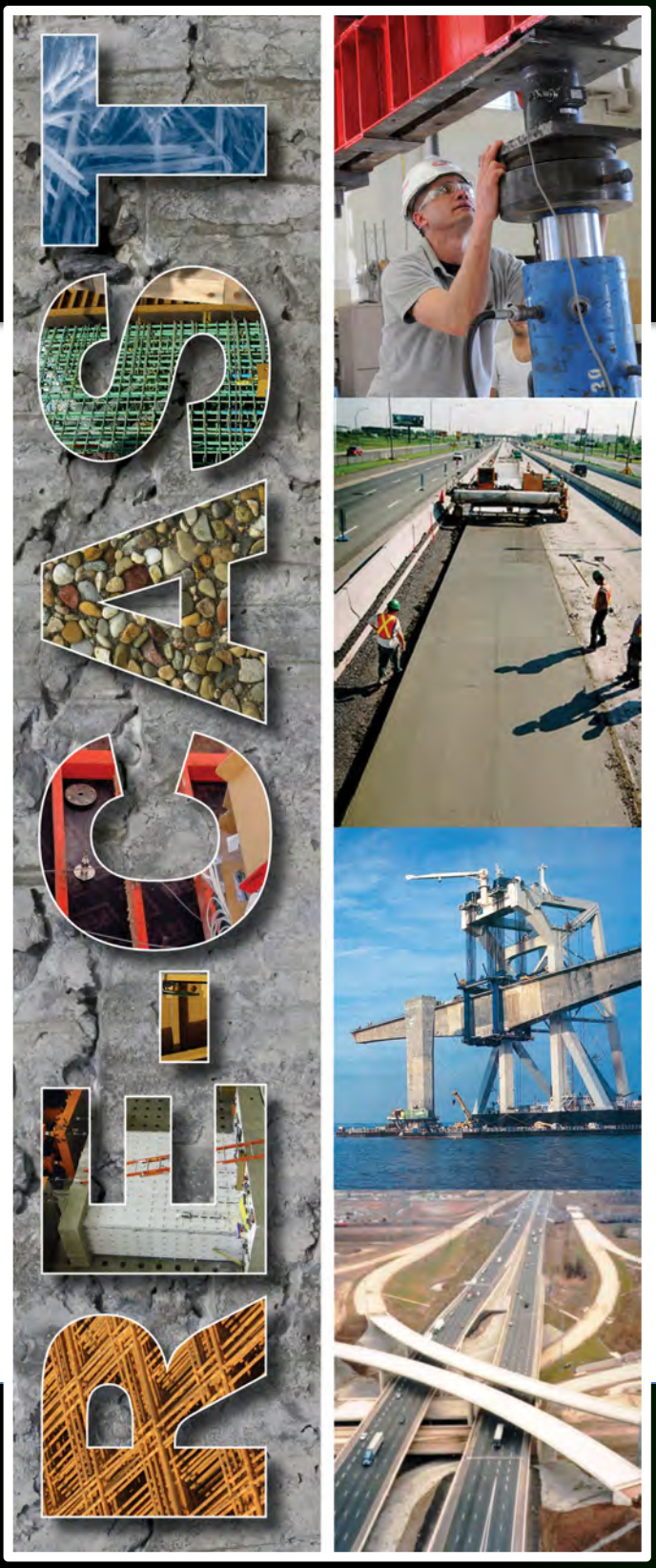

REsearch on Concrete Applications for Sustainable Transportation
Tier 1 University Transportation Center

FINAL PROJECT REPORT #00049223

GRANT: DTRT13-G-UTC45
Project Period: 12/1/2014 – 7/31/2019

Roller Compacted Concrete For Rapid Pavement Construction

Participating Consortium Member:
Missouri S&T

Authors:
Dr. Kamal H. Khayat
(Ph.D., P.Eng.) P.I.
Dr. Nicolas Ali Libre
(Ph.D.) Co-P.I.
Dr. Zemei Wu
(Ph.D.) Post-Doctoral Fellow

MISSOURI S&T
MIAMI
SOUTHERN UNIVERSITY AND A&M COLLEGE
RUTGERS

DISCLAIMER

The contents of this report reflect the views of the authors, who are responsible for the facts and the accuracy of the information presented herein. This document is disseminated under the sponsorship of the U.S. Department of Transportation's University Transportation Centers Program, in the interest of information exchange. The U.S. Government assumes no liability for the contents or use thereof.

TECHNICAL REPORT DOCUMENTATION PAGE

1. Report No. RECAST UTC #00049223	**2. Government Accession No.**	**3. Recipient's Catalog No.**
4. Title and Subtitle Roller Compacted Concrete for Rapid Pavement Construction		**5. Report Date** August 2019
		6. Performing Organization Code:
7. Author(s) Kamal H. Khayat, Nicolas Ali Libre, Zemei Wu		**8. Performing Organization Report No.** Project #00049223
9. Performing Organization Name and Address RE-CAST – Missouri S&T 500 W. 16th St., 223 ERL Rolla, MO 65409-0710		**10. Work Unit No.** **11. Contract or Grant No.** USDOT: DTRT13-G-UTC45
12. Sponsoring Agency Name and Address Office of the Assistant Secretary for Research and Technology U.S. Department of Transportation 1200 New Jersey Avenue, SE Washington, DC 20590		**13. Type of Report and Period Covered:** Final Report Period: 12/1/2014 – 7/31/2019 **14. Sponsoring Agency Code:**

15. Supplementary Notes
The investigation was conducted in cooperation with the U. S. Department of Transportation.

16. Abstract
The main objective of this research was to develop high-performance Roller Compacted Concrete (RCC) with enhanced solid skeleton to secure greater workability, mechanical properties, and frost durability. The study involved the development of a stepwise mixture design methodology to select aggregate proportioning and particle-size distribution of combined aggregates that can secure high packing density and lead to enhanced performance. RCC mixtures with high packing density of aggregate combination and suitable fresh and hardened properties were used to introduce air-entraining agent (AEA) at different dosages. The effect of binder content, AEA dosage, workability level, adjusted by varying the water-to-solid ratio, mixer type, and compaction energy on RCC performance was evaluated. Test results indicate that the performance of RCC can be improved with the increase in packing density of aggregate skeleton. Higher packing density can enable the reduction of cement content through improved compacted structure of the solid particles. RCC mixtures made with 40% sand, 20% intermediate aggregate, and 40% coarse aggregate lad to the highest packing density and best workability and mechanical properties. The binder content, workability level, and compaction technique were shown to considerably affect the mechanical properties, whereas the AEA dosage and mixer type had limited effect. The lowest 28-d compressive strength of 5220 psi (36 MPa) is greater than the 3500 - psi (24.1 - MPa) minimum strength for RCC pavement construction. The highest 28-d compressive strength was 8410 psi (58 MPa). The spacing factor of RCC mixtures was consistently below the targeted value of 0.009 in. (230 μm) with an air content lower than 7%. The RCC mixtures exhibited a durability factor greater than 70% after 123 freeze-thaw cycles and failed soon after, reflecting marginal frost durability. The incorporation of AEA significantly improved the salt-scaling resistance. The average mass loss of air-entrained RCC mixtures was lower than 11.8 oz/yd2 (400 g/m2) after 50 freeze-thaw cycles, which is considerably lower than the limit of 29.5 oz/yd2 (1000 g/m2).

17. Key Words Roller compacted, concrete	**18. Distribution Statement** No restrictions. This document is available to the public.	
19. Security Classification (of this report) Unclassified	**20. Security Classification (of this page)** Unclassified	**21. No of Pages** 99

Form DOT F 1700.7 (8-72) Reproduction of form and completed page is authorized.

Roller Compacted Concrete for Rapid Pavement Construction

Final Report

Investigators
Dr. Kamal H. Khayat, (Ph.D., P.Eng.) P.I.
Dr. Nicolas Ali Libre, (Ph.D.) co-P.I.
Dr. Zemei Wu, (Ph.D.) Post-Doctoral Fellow

ABSTRACT

The main objective of this research was to develop high-performance Roller Compacted Concrete (RCC) with enhanced solid skeleton to secure greater workability, mechanical properties, and frost durability. The study involved the development of a stepwise mixture design methodology to select aggregate proportioning and particle-size distribution of combined aggregates that can secure high packing density and lead to enhanced performance. RCC mixtures with high packing density of aggregate combination and suitable fresh and hardened properties were used to introduce air-entraining agent (AEA) at different dosages. The effect of binder content, AEA dosage, workability level, adjusted by varying the water-to-solid ratio, mixer type, and compaction energy on RCC performance was evaluated. Test results indicate that the performance of RCC can be improved with the increase in packing density of aggregate skeleton. Higher packing density can enable the reduction of cement content through improved compacted structure of the solid particles. RCC mixtures made with 40% sand, 20% intermediate aggregate, and 40% coarse aggregate lad to the highest packing density and best workability and mechanical properties. The binder content, workability level, and compaction technique were shown to considerably affect the mechanical properties, whereas the AEA dosage and mixer type had limited effect. The lowest 28-d compressive strength of 5220 psi (36 MPa) is greater than the 3500 - psi (24.1 - MPa) minimum strength for RCC pavement construction. The highest 28-d compressive strength was 8410 psi (58 MPa). The spacing factor of RCC mixtures was consistently below the targeted value of 0.009 in. (230 μm) with an air content lower than 7%. The RCC mixtures exhibited a durability factor greater than 70% after 123 freeze-thaw cycles and failed soon after, reflecting marginal frost durability. The incorporation of AEA significantly improved the salt-scaling resistance. The average mass loss of air-entrained RCC mixtures was lower than 11.8 oz/yd^2 (400 g/m^2) after 50 freeze-thaw cycles, which is considerably lower than the limit of 29.5 oz/yd^2 (1000 g/m^2).

Keywords: Air-entraining agent; Aggregate combination; De-icing salt scaling; Durability; Fresh properties; Freezing and thawing; Mechanical properties; Roller compacted concrete; Workability

ACKNOWLEDGEMENT

The authors would like to acknowledge the REsearch on Concrete Applications for Sustainable Transportation (RE-CAST), a Tier-1 University Transportation Center at Missouri University of Science and Technology (Missouri S&T) as well as the Missouri Department of Transportation (MoDOT) for providing the financial support.

The authors also take this opportunity to express a deep sense of gratitude to Mr. William Stone and Ms. Jennifer Harper from MoDOT for their cordial support throughout this project. The authors are also grateful to Mr. Austin Kramer, Dr. Iman Mehdipour, and Dr. Seyedhamed Sadati for their assistance in conducting the tests. We also acknowledge the support of Mr. Jason Cox for his valuable technical support in the laboratory work. The cooperation and support from Ms. Abigayle Sherman and Gayle Spitzmiller, staff members at the Center for Infrastructure Engineering Studies (CIES), is greatly acknowledged.

EXECUTIVE SUMMARY

The main goal of this project was to develop a mixture proportioning approach for high-performance RCC for rapid pavement construction. The approach involved the optimization of the aggregate composition that can enhance workability of the “zero-slump” RCC and securing an adequate air-void system and hence proper frost durability, which remains a challenging factor in such dry concrete material.

In total, 17 different aggregates of different nominal maximum sizes and types were selected, and their physical properties, including the gradation, shape, texture, water absorption, and packing density values were evaluated. Seventeen aggregate combinations with different proportions of fine, intermediate, and coarse aggregates were then investigated to achieve maximum possible packing density values using a statistical mixture design (SMD) method. Key fresh and hardened properties of the RCC mixtures made with the 17 different aggregate proportions and a fixed water-to-cementitious ratio (w/cm) of 0.4 were determined. Optimized RCC mixtures with optimal aggregate combinations that showed the optimal packing density and satisfactory fresh and hardened properties were used to introduce air-entrained agent (AEA) of different dosage rates. In total, 11 air-entrained RCC mixtures were investigated.

The investigation also involved the evaluation of the effect of the binder content, AEA dosage, Vebe workability level, mixer type, and compaction energy on mechanical properties and durability. The durability results of the developed RCC mixtures were compared to those of three reference mixtures developed in the field and from previous laboratory research carried out by the authors in collaboration with MoDOT in 2013. Based on the findings of this research, the main findings are summarized below.

(1) Selection and optimization of aggregate combination

In total, 17 aggregate combinations with different nominal maximum sizes (fine, intermediate [or pea gravel], and coarse) and shapes (crushed and rounded) were selected. The packing densities of the aggregates were determined using the gyratory intensive compaction tester (ICT). The aggregate combinations having different proportions of fine, intermediate, and coarse aggregates were evaluated. The possible maximum packing density values that can be obtained for different aggregate combinations were determined using statistical mixture design (SMD) method. Table 1 summarizes the proportions of 17 aggregate combinations used for the SMD approach. The ternary diagrams for packing density of aggregate combinations that were established using the SMD approach and those obtained from a packing model are shown in Figure 1.

Table 1 Proportions of 17 aggregate combinations used for the SMD approach

Mix #	Aggregate ratio (mass)		
	Sand	Intermediate aggregate	Coarse aggregate
R1	40%	20%	40%
R2	40%	10%	50%
R3	40%	30%	30%
R4	50%	10%	40%
R5	50%	20%	30%
R6	60%	10%	30%
R7	30%	20%	50%
R8	30%	30%	40%
R9	60%	0%	40%
R10	60%	20%	20%
R11	50%	30%	20%
R12	44%	18%	38%
R13	20%	20%	60%
R14	20%	30%	50%
R15	30%	10%	60%
R16	30%	40%	30%
R17	40%	15%	45%

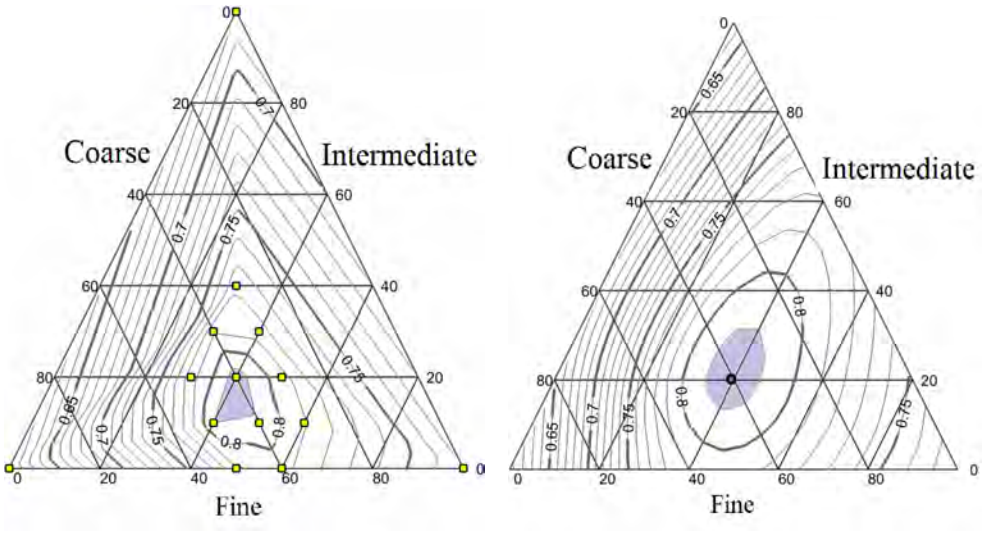

(a) Packing density (b) Toufar packing density model

Figure 1 Ternary diagrams of aggregate packing density

The main findings from the first phase of the research dealing with the selection and optimization of aggregate combinations can be summarized as follows:

- The packing density of aggregate can vary with the nominal maximum size, shape, surface texture, and angularity of the aggregate.
- The packing densities of the investigated fine, intermediate, and coarse aggregates vary in the range of 0.58 - 0.72, 0.60 - 0.68, and 0.59 - 0.61, respectively.
- Given different aggregate combinations and proportions, the packing density (Φ) of the investigated ternary aggregate combinations varied from 0.63 to 0.82. The optimal aggregate combination for the selected aggregates was found to consist of 40% sand, 20% intermediate aggregate, and 40% coarse aggregate, resulting in a high packing density of more than 0.8.
- Regardless of the aggregate type, the packing density of blended aggregate increased with the increase in fine-to-total aggregate ratio up to a certain threshold value, beyond

which the maximum packing density decreased with further increase in fine aggregate replacement.

- The void ratio (1-Φ) corresponds to the minimum volume of paste needed to fill the voids between aggregate particles. The void ratio of the selected aggregate combinations varied from 0.37 to 0.28. This indicates that the minimum paste content can be reduced by 32% by optimizing the aggregate combinations to reduce the void ratio, hence resulting in more cost-effective RCC mixtures.

(2) Performance evaluation of non-air-entrained RCC mixtures with different aggregate combinations

Cementitious materials were then mixed with the 17 aggregate combinations to prepare non-air-entrained RCC mixtures with a fixed water-to-cementitious ratio of 0.40 and a cement content of 520 lb/yd^3 (309 kg/m^3). Key fresh and hardened properties, including the Vebe time, the proposed segregation index, as well as the compressive strength and the bulk electrical resistivity of the RCC mixtures at ages of 7, 14, 21, and 28 d, were investigated. The Vebe time and segregation index are shown in Figure 2. Figure 3 depicts the 28-d compressive strength and 14-d electrical resistivity ternary diagrams of the investigated RCC mixtures.

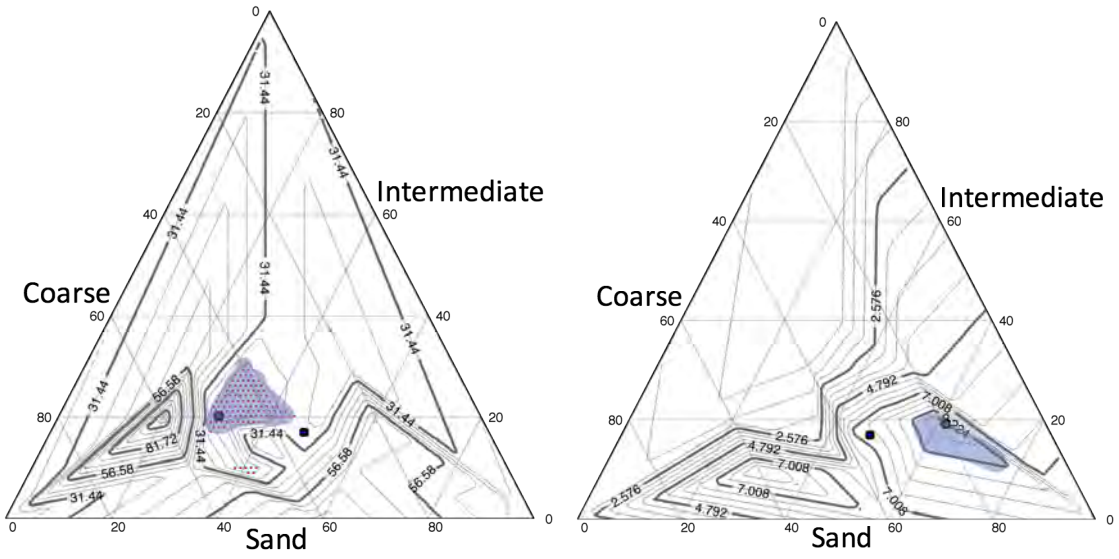

(a) Vebe time (b) Segregation index

Figure 2 Ternary diagrams of fresh properties of non-air-entrained RCC mixtures made with different aggregate combinations

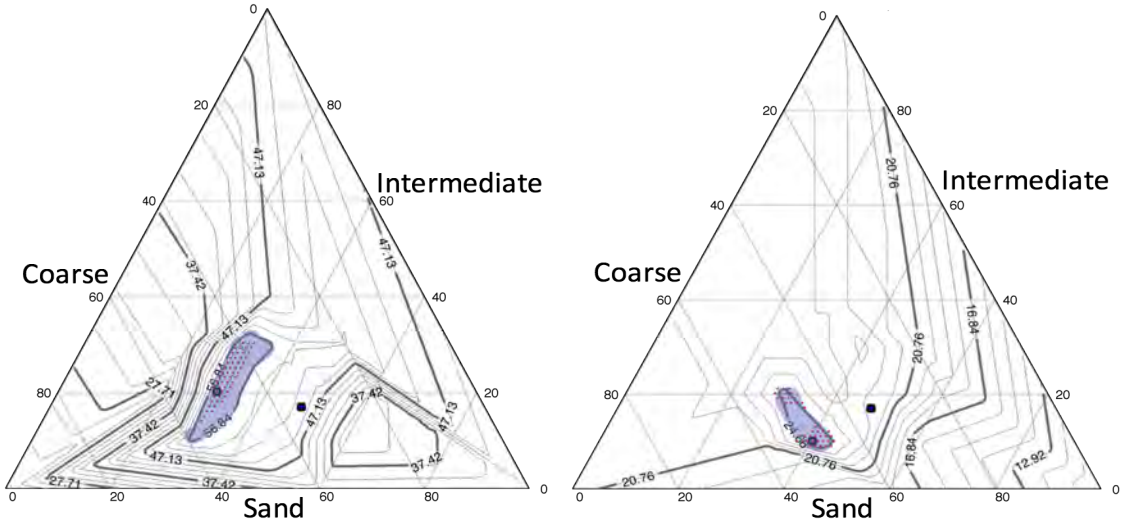

(a) 28-d compressive strength (b) 14-d electrical resistivity

Figure 3 Ternary diagrams of 28-d compressive strength and 14-d electrical resistivity of non-air-entrained RCC mixtures

Based on the results obtained from the second phase, the following conclusions can be drawn:

- Increasing the sand content in RCC mixtures was shown to increase the Vebe time (reduced workability). The risk of segregation of the RCC mixture was also increased by increasing the sand and intermediate aggregate contents.
- All compressive strength values were greater than the minimum value of 3500 psi (24.1 MPa) required for RCC pavement construction. The highest strength and surface resistivity values were obtained for aggregate combinations corresponding to the highest packing density.
- RCC mixture made with 40% coarse aggregate, 20% intermediate aggregate, and 40% sand had the highest packing density and the best workability, strength, and electrical resistivity.

(3) Investigation of air-entrained RCC mixtures

The optimized non-air-entrained RCC mixture with 40% coarse aggregate, 20% intermediate aggregate, and 40% sand was selected to investigate the effect of air-entrained agent (AEA) dosage (8, 16, and 32 oz/yd^3) [309, 619, and 1238 ml/m^3], binder content (430, 510, and 580 lb/yd^3) [255, 303, 344 kg/m^3], workability level (Vebe time of 15 - 30, 30 - 60, and 60 - 90 s), mixer type (Omni, Drum, and Eirich high shear mixer), and compaction technique (Vibrating hammer, Vebe vibrating table, and intensive compaction technology) on mechanical properties and durability. The results of the compressive strength at 7 and 28 days and surface resistivity at 7 to 28 days of 11 air-entrained RCC mixtures are summarized in Table 2. The results of the air-void system, including spacing factor, air content, and specific volume, are summarized in Table 3.

Table 2 Compressive strength and surface resistivity of air-entrained RCC mixtures

Mix #	Compressive strength, psi (MPa)		Surface resistivity (kΩ.cm)			
	7 d	28 d	7 d	14 d	21 d	28 d
AH	5210 (35.9)	7800 (53.5)	24	26	31	34
AM	5550 (38.3)	7800 (53.8)	25	27	34	35
AV	5730 (39.5)	7400 (51.0)	25	28	32	36
BL	3870 (26.7)	5220 (36.0)	19	25	26	28
BH	4840 (33.4)	8400 (57.9)	22	24	32	33
WL	5610 (38.7)	7990 (55.1)	22	24	31	34
WH	3190 (22.0)	6540 (45.1)	16	22	22	24
MO	5670 (39.1)	8290 (57.2)	24	29	29	33
MH	5240 (36.1)	7900 (54.5)	23	28	29	32
CV	3870 (26.7)	6540 (45.1)	18	22	23	29
CH	5410 (37.3)	7610 (52.5)	23	26	30	32

Table 3 Air-void system results of air-entrained RCC mixtures

Mix #	Spacing factor (μm)			Air content (%)			Specific volume (mm^2/mm^3)					
	1	2	Ave.	1	2	Ave.	< 0.5 mm	< 0.5 mm	Ave.	< 1.0 mm	< 1.0 mm	Ave.
AH	186	152	169	4.9	7.1	6.0	25.7	19.8	22.8	16.1	13.7	14.9
AM	251	196	224	4.8	5.2	5.0	16.7	18.6	17.7	13.2	14.6	13.9
AV	257	172	215	7.5	6.6	7.1	18.3	24.0	21.2	9.2	19.0	14.1
BL	173	130	152	7.2	6.5	6.9	19.2	31.1	25.2	13.6	12.8	13.2
BH	137	210	174	7.4	4.4	5.9	21.2	21.5	21.4	15.3	16.0	15.7
WL	95	176	136	4.4	7.4	5.9	41.2	17.5	29.4	30.6	12.1	21.4
WH	63	73	68	16.4	9.6	13.0	23.0	28.0	25.5	15.8	21.6	18.7
MO	106	131	119	4.3	7.5	5.9	33.3	26.6	30.0	25.7	20.0	22.9
CH	158	157	158	5.7	4.1	4.9	23.1	29.6	26.4	29.6	23.0	26.3

Based on the findings from the third phase, the following conclusions are warranted:

- The 28-d compressive strengths of the 11 tested mixtures exceeded 5220 psi (36.0 MPa). This meets the strength requirement of RCC for pavement construction. The values of surface resistivity of all the RCC mixtures ranged from 9.4 to 14.2 kΩ.in. (24 to 36 kΩ.cm), which can be classified as moderate and/or low penetrability index values.

- For a given binder content, the increase in AEA dosage from 8 to 32 oz/yd^3 (309 to 1238 ml/m^3), by volume of concrete, slightly decreased the 28-d compressive strength and electrical resistivity.
- The increase of the binder content resulted in greater compressive strength. For example, increasing the binder content from 430 lb/yd^3 (255 kg/m^3) to 580 lb/yd^3 (344 kg/m^3) led to 28-d compressive strength varying from 5220 psi (36 MPa) to 8340 psi (57.8 MPa), corresponding to 61% increment.
- The proportioning of RCC with high workability level (Vebe time of 15 - 30 s) that was achieved by adjusting the water-to-solid ratio decreased the 7- and 28-d compressive strengths by 41% and 18%, respectively, compared to RCC with low workability level (Vebe time of 60 - 90 s). The surface resistivity of the former mixture was also reduced by 10% to 42%, depending on curing age.
- The mixer types with different shear energies used to prepare the RCC mixtures had limited effect on compressive strength and surface resistivity of RCC. The two RCC mixtures prepared using the Omni and Eirich high shear mixers had similar 28-d compressive strength and 28-d surface resistivity results of 7250 psi (55 MPa) and 12.6 kΩ.in. (32 kΩ.cm), respectively.
- The compaction technique used to consolidate RCC test specimens had a significant effect on mechanical properties. RCC specimens that were vibrated manually using a vibrating hammer had 7- and 28-d compressive strength values of 5410 psi (26.7 MPa) and 7610 psi (52.5 MPa), respectively, which were 41% and 16% greater than those of the mixture compacted using the Vebe vibrating table. The surface resistivity values of

the former compaction technique were 18% - 30% greater at different ages, indicating denser structure.

- Proper spacing factor below 0.009 in. (230 μm) was achieved for the developed air-entrained RCC mixtures. The hardened properties and air-void system of the RCC mixtures with less workability were improved compared to the one with high workability. The 28-d compressive strength and electrical resistivity of the mixture with low workability were improved by 18% and 29%, respectively. Its air content was decreased by 55%.

(4) Durability of optimized air-entrained RCC mixtures

Four of the optimized air-entrained RCC mixtures were selected for durability testing. In order to compare the durability characteristics of the investigated RCC mixtures, three additional admixtures, including a non-air-entrained RCC used for the construction of Route 160 (RF) near Doniphan, MO in 2013, a reference mixture without any air entrainment (RN), and an air-entrained RCC mixture with 44 oz/yd^3 (1707 ml/m^3) AEA (RA) developed by the authors and used in a previous RCC research project with MoDOT were selected. Figure 4 compares the durability factor of the investigated RCC mixtures and the RF mixture taken from the field. Figure 5 presents the cumulative mass loss of the four developed RCC admixtures and the RN and RA mixtures up to 50 freeze-thaw cycles of salt-scaling testing.

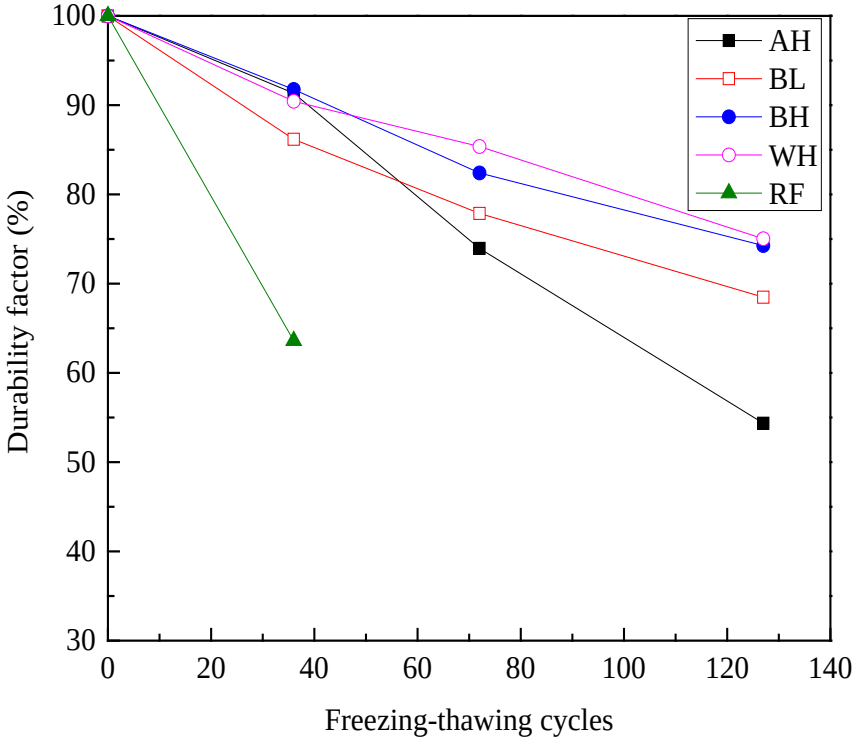

Figure 4 Durability factor of investigated RCC mixtures

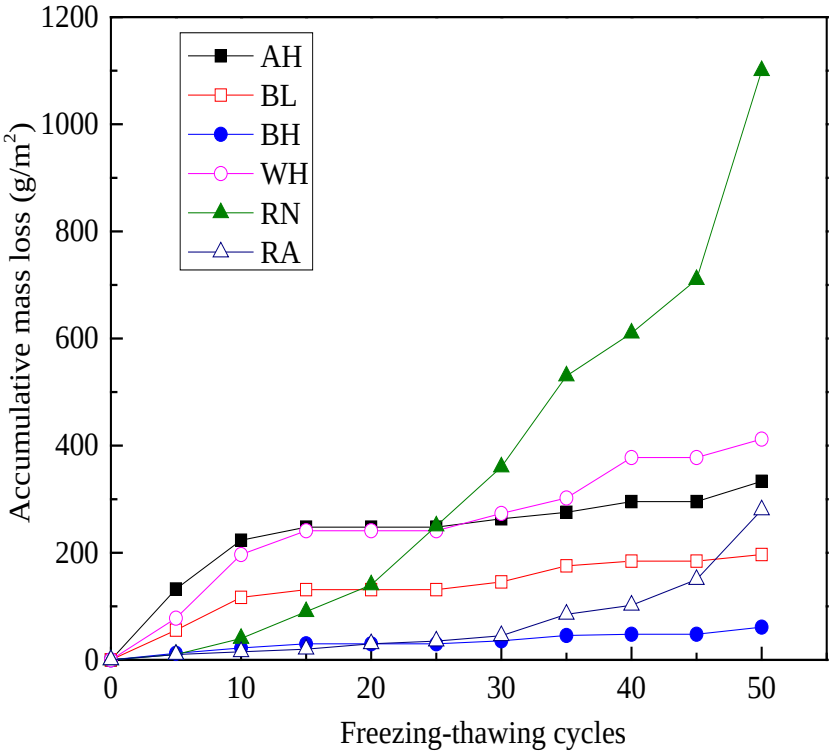

Figure 5 Cumulative mass loss of the RCC mixtures during salt scaling testing

Based on the results from the durability test, the following main findings can be established:

- The non-air-entrained RCC mixture used for the experimental field construction in 2013 showed a low durability factor of 63% after only 36 freeze-thaw cycles; the test specimens cracked soon after. The four optimized air-entrained RCC mixtures had better frost resistance with durability factors of approximately 70% after 123 freeze-thaw cycles. However, some specimens failed at this cycle and the testing was stopped.
- The de-icing salt scaling mass loss of the reference mixture without air-entrainment was noticeably higher than other mixtures, especially after 30 cycles, which was 10.6 oz/yd^2 (360 g/m^2). The cumulative loss after approximate 35 cycles was over 17.7 oz/yd^2 (600 g/m^2).
- The air-entrained RCC mixtures exhibited good salt-scaling resistance with average mass loss lower than 11.8 oz/yd^2 (400 g/m^2) after 50 cycles, which meets the limit of 29.5 oz/yd^2 (1000 g/m^2).

TABLE OF CONTENTS

LIST OF FIGURES

LIST OF TABLES

1. INTRODUCTION

1.1. Problem statement

The American Concrete Institute (ACI) defines roller compacted concrete (RCC) as a concrete of zero-slump in its unhardened state that is typically transported, placed, and compacted using earth and rockfill construction equipment (ACI, 2010). RCC has the same basic ingredients as conventional concrete, including cement, water, and aggregates, such as gravel or crushed stone. Compared to conventional concrete, RCC typically contains less cementitious materials, higher aggregate content, and less water and paste content.

The application of RCC in pavements has become increasingly viable because of the beneficial characteristics of such concrete. RCC with zero slump is placed with conventional or high-density paving equipment and compacted using rollers, hence eliminating the need of forms during placement and need for finishing procedure, hence increasing the speed of construction. The use of RCC can increase early strength development that allows constructed pavements to be opened to traffic at earlier age. Reducing the construction duration and enhancing early-age and long-term performance, are the key solutions for decreasing direct and indirect costs. Given the high aggregate content of RCC, such concrete can develop relatively low drying shrinkage.

The incorporation of an air-entraining admixture (AEA) in concrete is necessary to enhance frost durability, including the resistance to de-icing salt scaling. However, the incorporation of AEA in a zero-slump concrete, such as RCC, is quite challenging and can lead to inconsistent performance under freezing and thawing conditions. RCC mixtures that are properly air-entrained have been shown to develop proper frost durability under standard laboratory testing conditions (Liu, 1991). However, due to low the cement paste content and low workability of RCC, it is quite difficult to provide a sufficient amount of air entrainment to

ensure uniform distribution of closely spaced and tiny air bubbles to secure adequate air-void system.

The authors at Missouri University of Science and Technology (Missouri S&T) have conducted research in collaboration with the National University Transportation Center (NUTC) and Missouri Department of Transportation (MoDOT) to investigate the performance of RCC in pavement construction. In-situ properties of RCC used for Route 160 in Doniphan, MO, showed acceptable performance of RCC mixtures in pavement construction (Khayat and Libre, 2014). Table 1.1 summarizes the mechanical properties of the RCC mixtures sampled during the casting of the RCC as well as those of an optimized RCC mixture that was air-entrained developed in the first phase of that research project. The study observed that the 7-day compressive strength of the RCC mixtures was greater than 3,600 psi (25.0 MPa), indicating the possibility of opening traffic at early age. The 28-day compressive strength was higher than 3,500 psi (24.1 MPa), which is the minimum strength required by MoDOT for pavement construction. Both in-situ and laboratory monitoring of drying shrinkage revealed that its shrinkage values were considerably lower than those of conventional concrete used for pavement construction. This can lead to an increase in saw-cut spacing to control shrinkage cracking of RCC pavement. The RCC developed relatively high modulus of elasticity, and adequate splitting tensile and flexural strengths. On the other hand, the durability characteristic of RCC determined by surface resistivity, volume of permeable voids, deicing salt scaling resistance, and freezing and thawing resistance showed that frost resistance of RCC is a controversial topic. Even though the laboratory optimized air-entrained RCC mixture offered much better frost durability than that of the field-cast non-air-entrained RCC, the concrete did not satisfy the general requirement for frost durability that is expected for conventional concrete used in pavement construction.

Therefore, further investigation is needed to develop RCC mixtures that can secure adequate frost durability. This can involve the development of high-performance RCC mixtures with high packing density of the aggregate skeleton to achieve high strength and impermeability that can enhance frost durability as well as the combination of such an approach with the entrainment of an adequate air-void system to enhance strength and durability characteristics.

Table 1.1. Performance comparison of reference and optimized RCC mixtures

Properties test	RCC, Route 160	Optimized RCC
7-day compressive strength, psi (MPa)	3600 (25.0)	6200 (42.7)
28-day compressive strength, psi (MPa)	4200 (29.0)	6800 (46.9)
28-day splitting tensile strength, psi (MPa)	420 (2.9)	450 (3.1)
91-day flexural strength, psi (MPa)	630 (4.3)	820 (5.6)
91-day modulus of elasticity, ksi (GPa)	4500 (31.0)	5500 (37.9)
Shrinkage deformation (με) after 300 days	400	300

1.2. Research objectives

The study aimed at developing RCC with improved packing density, strength, and frost durability that can be used in rapid pavement construction. The mixture proportioning approach involves the optimization of the aggregate combinations and the entrainment of proper air-void system to enhance workability, mechanical properties, and frost durability. The specific objectives of this project are described as follows:

- Investigate various RCC mixtures prepared using locally available materials in Missouri.
- Optimize RCC mixture proportions to secure satisfactory workability, mechanical properties, and frost durability.

1.3. Research methodology

The research project includes the following tasks:

(1) Background information regarding RCC mixture design and performance;

(2) Optimization of aggregate combination;

(3) Optimization of air-entrained RCC mixtures;

(4) Recommendation of RCC mixture proportioning for field implementation.

Further details of the work tasks are described below.

1.3.1. Task 1 – Background information regarding RCC mixture design and performance

Various RCC mixture proportion techniques used for laboratory research and field projects were collected and compared to determine the range of optimum RCC mixtures in pavement applications. Different techniques developed for RCC mixture optimization were reviewed. Findings indicate that there are novel trends on mixture optimization of RCC through optimized particle size distribution (PSD) to enhance packing density. As expected, previous studies revealed that the aggregate combination plays a crucial role in optimization of RCC.

The effect of PSD on workability and compactibility of fresh RCC and mechanical properties of the hardened concrete were summarized. In addition, the durability of RCC mixtures was reviewed. This includes durability to freezing and thawing, de-icing salt scaling, and abrasion damage.

1.3.2. Task 2 – Optimization of aggregate combination

Aggregate accounts for 75% - 85% of the total volume of the RCC mixtures and their characteristics can greatly affect fresh and hardened properties of the material. Coarse aggregate may either be crushed or rounded. Fine aggregate can be natural or manufactured or a combination of the two. Crushed aggregates are typically preferred for RCC given the enhanced

aggregate interlock and positive effect on mechanical properties. Crushed coarse aggregate can improve compressive and flexural strengths of concrete and reduce the risk of segregation. However, concrete mixtures made with crushed aggregate can develop lower workability.

Both rounded and crushed aggregates, representing aggregates available in Missouri, were investigated to study the effect of aggregate characteristics on the performance of RCC. Key aggregate characteristics, including shape, nominal maximum size, density, abrasion resistance, PSD, and packing density were examined in this Task. These characteristics were related to the evaluated key performance of RCC.

In Task 2, three Subtasks, including the testing of various aggregate combinations, the development of grading requirements, and performance evaluation of non-air-entrained RCC made with different aggregate combinations were sequentially investigated, as indicated below.

Subtask 2.1 Testing of various aggregate combinations

Previous studies on RCC confirm that the selection of a proper aggregate combination to achieve high packing density is crucial in optimizing the PSD for RCC. Such optimization, however, depends on the physical properties of aggregate that vary with aggregate type and source. In this research project, 17 different aggregates were selected to cover a wide range of materials available in Missouri. Their optimum combinations were determined using different approaches.

Subtask 2.2 Developing grading requirements

The experimental results obtained in Subtask 2.1 were analyzed and compared with theoretical packing models to develop a protocol for reliable selection of aggregate combinations that can be used for RCC pavement construction. The developed protocol takes into account theoretical packing models as well as experimental measurements for pre-qualifying the

aggregates and optimization of the PSD. Grading requirements were developed to achieve the highest packing density for typical aggregate available in Missouri.

In addition, other grading parameters, such as the risk of segregation, compactibility of the aggregate, and workability of concrete produced by such aggregate combinations, were considered in proposing aggregate gradation. Coarse aggregates are prone to segregation in a dry and low-paste content RCC. Therefore, aggregate combinations should be finely tuned so that the mixture has sufficient resistance against separation of the coarse aggregate from the fine particles. Therefore, the grading requirement for combined aggregate was verified to check its compliance with segregation resistance requirements.

The compactibility of solid particles was considered in the research program. The compactibility parameter measures the energy consumed by compacting a certain RCC mixture, which should be minimized to reduce the effort required for RCC construction.

Subtask 2.3 Performance evaluation of non-air-entrained RCC mixtures made with different aggregate combinations

The results from the selected aggregate combinations were used to prepare RCC mixtures without any air entrainment. The RCC mixtures were tested for workability (Vebe time), surface electrical resistivity, density, and compressive strength to secure high packing density RCC mixtures. The benefits of using aggregate combinations with optimized PSD to reduce cement content and improve mechanical properties concrete pavement were also investigated.

1.3.3. Task 3 – Optimization of air-entrained RCC mixtures

The preliminary study of this research project showed that air entrainment can be introduced in the RCC mixtures. However, adjusting the amount of air content, the stability of air bubbles during the transport and compaction, as well as uniformity of air-void distribution across

the pavement are important challenges that should be addressed when using air-entrained RCC. The goal of this task was to develop production techniques to adjust the amount of entrained air in RCC. The uniformity of the air-void system was also investigated.

Studied parameters affecting air-void system of air-entrained RCC and hardened concrete performance validation are presented in Subtasks 3.1 and 3.2, respectively.

Subtask 3.1 Study parameters affecting air-void system of air-entrained RCC

The investigated parameters included:

- The incorporated AEA dosage (medium, high, and very high);
- Workability level changed by altering the water-to-solid ratio to secure Vebe times of 90 - 60, 60 - 30, and 15 - 30 s;
- Binder volume (low, medium, and high);
- Mixer type (Omni mixer, drum mixer, and Eirich high shear mixer);
- Compaction technique (vibrating hammer, Vebe vibrating table, and gyratory intensive compaction tester [ICT]).

Table 1.2 summarizes the mixture design parameters that were considered in this study. Due to difficulties in measuring the air content of very dry concrete, core samples were taken to measure the air-void system of the hardened concrete according to ASTM C 457.

Subtask 3.2 Hardened concrete quality validation

Hardened concrete specimens were taken from the investigated mixtures to determine compressive strength, surface electrical resistivity, spacing factor, and air-void content and volume. For the selected mixtures for durability characterization, further testing was conducted to evaluate the splitting tensile strength, modulus of elasticity, permeable void, water absorption,

frost durability, and resistance to de-icing salt scaling. Table 1.3 summarizes the testing methods used in Tasks 2 and 3.

Table 1.2. Matrix experiment of Tasks 2 and 3

Mixture	Binder volume			Workability level (VEBE TIME)			Mixer type			Compaction technique			AEA dosage		
	Low (430 lb/yd^3)	Medium (510 lb/yd^3)	High (580 lb/yd^3)	Low (60-90 s)	Medium (30-60 s)	High (15-30 s)	Omni	Drum	Eirich	Vibrating hammer	Vebe vibrating table	ICT	Medium (8 oz/yd^3)	High (16 oz/yd^3)	Very high (32 oz/yd^3)
AEA dosage level															
AM		x			x			x				x	x		
AH		x			x			x				x		x	
AV		x			x			x				x			x
Binder volume															
BL	x				x			x				x		x	
BH			x		x			x				x		x	
Workability level															
WL		x		x				x				x		x	
WM		x			x			x				x		x	
WH		x				x		x				x		x	
Mixer type															
MO		x			x		x					x		x	
MD		x			x			x				x		x	
MH		x			x				x			x		x	
Compaction technique															
CH		x			x			x		x		x		x	
CV		x			x			x			x			x	

Table 1.3. Proposed concrete testing methods

Property	Test Method	Test Title/Description
Fresh Concrete Property Tests		
Vebe time	ASTM C1170	Standard Test Method for Determining Consistency and Density of Roller-Compacted Concrete Using a Vibrating Table
Hardened Mechanical Property Tests		
Density	ASTM C 642	Standard Test Method for Density, Absorption, and Voids in Hardened Concrete
Compressive strength	ASTM C 109	Standard Test Method for Compressive Strength of Hydraulic Cement Mortars (Using 2-in. or [50-mm] Cube Specimens)
Splitting tensile strength	ASTM C 496	Standard Test Method for Splitting Tensile Strength of Cylindrical Concrete Specimens
Modulus of elasticity	ASTM C 469	Standard Test Method for Static Modulus of Elasticity
Durability Tests		
Surface electrical electricity	AASHTO T95	Standard Method of Test for Surface Resistivity Indication of Concrete's Ability to Resist Chloride Ion Penetration
Permeable void	ASTM C 642	Standard Test Method for Density, Absorption, and Voids in Hardened Concrete
Freeze-thaw resistance	ASTM C 666	Standard Test Method for Resistance of Concrete to Rapid Freezing and Thawing (Procedure A)
Spacing factor (L)	ASTM C 457	Standard Test Method for Microscopical Determination of Parameters of the Air-Void System in Hardened Concrete
Scaling resistance	ASTM C 672	Standard Test Method for Scaling Resistance of Concrete Surfaces Exposed to Deicing Chemicals

1.3.4. Task 4 – Recommendation of RCC mixture proportioning for field implementation

The goal of this task was to provide guidelines for the selection of concrete constituent materials, mixture optimization methodology, and performance-based specifications for RCC based on the outcome of the research. The results from this research can contribute to the development and implementation of new mixture design methodology and quality control tools for the design and construction of concrete pavement using RCC. The use of RCC can accelerate

concrete pavement construction and improve mechanical and long-term performance, leading to reduced life-cycle cost of the transportation infrastructure.

1.4. Outline

This report consists of six sections. Section 1 reviews some of the challenges in designing zero-slump RCC with proper incorporation of AEA and frost durability for pavement constructions and elaborates the objectives and scope of the research work and methodology. A brief background of RCC characteristics, including the effect of PSD of aggregate on workability and mechanical properties is presented in Section 2. The constituent materials, mixture design, mixing procedure, testing program, and test methods are described in Section 3. Section 4 presents the fresh and hardened properties of RCC mixtures with optimized aggregate combination and adequate air-void system. In total, 17 RCC mixtures were proportioned with different types and combinations of aggregate. Focus was placed to secure high packing density and satisfactory fresh and mechanical properties of the RCC mixtures. The optimal aggregate skeleton was used to prepare 11 air-entrained RCC mixtures and compare their mechanical property and durability characteristics to those of three reference mixtures developed from a previous project carried out by the authors and MoDOT.

Section 5 presents the recommendation of RCC mixture proportions that can be used for field implementation. Section 6 summarizes the main findings obtained from this research and presents proposed perspectives for future studies.

2. Task 1 - BACKGROUND

2.1. Introduction

Pavement design strength, durability requirements, and intended application affect the selection of materials in RCC pavement construction. Therefore, special attention is required to select material constituents and mixture design to ensure the selected RCC mixtures meet the design and performance criteria.

Aggregate properties affect the workability, compactibity under vibratory action, and hardened properties. Proper selection of suitable aggregates can result in greater economy in construction and longer serviceability of RCC pavements. Aggregates should generally meet the quality requirements of ASTM C33 and Missouri Standard Specifications for Highway Construction (2004).

Some specifications present the minimum cement and/or cementitious contents, as well as the maximum supplementary cementitious material (SCM) replacement percentages. Missouri Standard Specifications for Highway Construction (2004) requires that the total amount of cementitious materials shall not be below 400 lb/yd^3 (237 kg/m^3). The maximum fly ash replacement level should be limited to 25%, by mass of total binder, in order to prevent scaling of the concrete pavement surface. The ground granulated blast furnace slag (GGBFS) and silica fume contents should not exceed 8% and 30%, respectively.

Regardless of mixture proportioning method or concrete type, all concrete mixtures should comply with certain requirements. Constructability, mechanical and durability characteristics, and economical aspects are the major influencing factors in mixture proportioning of concrete. In addition, the RCC mixture proportions should also be properly adjusted to ensure long-term performance. The major influencing factors that are usually

considered in the RCC mixture proportioning are summarized in Table 2.1. Missouri Standard Specifications for Highway Construction (2004) requires that 28-d compressive strength of RCC mixtures should be at least 3,500 psi (24 MPa) when specimens are prepared according to ASTM C 1176 or ASTM C 1435.

Table 2.1. Factors affecting mixture proportioning of RCC

Constructability	Mechanical properties	Economics	Durability
Required density with optimal compaction effort	Compressive and flexural strengths should meet design criteria	Use of locally available materials	Controlled shrinkage
Workable enough		Lower cement consumption	Low cracking and water permeability
No segregation		Use of SCM	Good abrasion resistance

RCC has a lower paste volume and water content; therefore, it is much drier than conventional pavement concrete and has low workability. RCC requires a larger fine aggregate content to produce a combined aggregate that is well-graded and stable under the action of a vibratory roller (Harrington et al. 2010). RCC is generally not air-entrained because proper formation and distribution of air-bubbles in a very dry mixture RCC are challenging. However, RCC pavement in cold regions subjected to freeze-thaw action and deicing salt scaling should be durable. Minimizing frost damage in RCC has been achieved by proportioning mixtures with sufficiently low water-to-cementitious materials ratio (w/cm) to reduce permeability of the cement paste. Proper use of AEA is challenging given the limited water content in RCC. Research work on very dry concrete mixtures, including RCC, can require 5 to 10 times greater dosage of AEA than that of conventional concrete to secure a given air content (Hazaree et al.

2011). However, the practicality of producing air-entrained RCC in the field has not yet been demonstrated.

2.2. Effect of PSD of aggregates on properties of RCC

RCC usually contains more aggregate (75% to 85% by volume) and less paste compared to conventional concrete. Therefore, aggregate properties significantly affect both the fresh and hardened characteristics of RCC. In freshly mixed RCC, aggregate characteristics affect the workability and its potential to segregate and the ease with which it will properly consolidate under a vibratory roller. RCC mixtures made with different aggregate combinations of continuous PSD can develop greater packing density, thus requiring less cement demand for given workability. The strength, modulus of elasticity, thermal properties, and durability of the hardened RCC are also affected by the aggregate properties. Therefore, the optimization of aggregate characteristics plays a major factor in producing high-quality RCC. Suggested grading limits of combined coarse and fine aggregate in accordance with ACI 325 and PCA that have been used to produce satisfactory RCC pavement are shown in Figure 2.1. The different gradation requirement comes from the need of the RCC aggregate skeleton to be effectively consolidated under compaction efforts from the paver and to ensure segregation resistance.

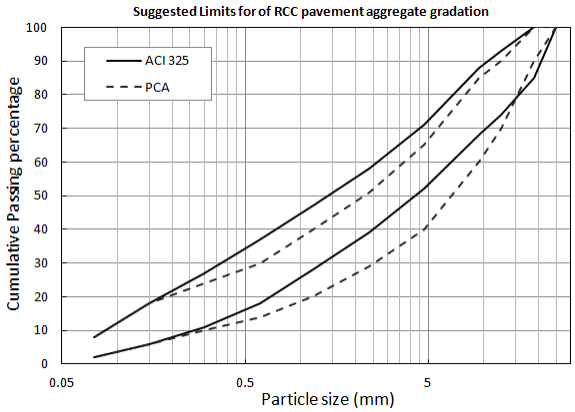

Figure 2.1. Suggested limits of aggregate gradation for RCC pavement

As specified in Missouri Standard Specifications for Highway Construction (2004), the aggregate used in RCC shall be well-graded without gradation gaps and the PSD of combined aggregates should conform to the limits as given in Table 2.2.

Table 2.2. Combined aggregate gradation limit

Sieve size	Percentage passing, by mass
1 in. (25.4 mm)	100%
1/2 in. (12.7 mm)	70% - 90%
3/8 in. (9.5 mm)	30% - 85%
No. 4 (4.76 mm)	40% - 60%
No. 200 (75 μm)	0 - 8%

2.2.1. Workability and compactibility

The PSD of the granular materials is one of the primary parameters to ensure proper consolidation of fresh concrete under roller vibration and preventing aggregate segregation during transportation and placement. RCC often requires greater fine aggregate content and lower coarse aggregate content than conventional pavement concrete. In order to ensure a dense, smooth, and high-quality surface of RCC, well-graded aggregate combinations with adequate packing density should be employed to secure mixtures with low paste content, hence minimizing the void space and reducing the risk of segregation.

Concrete made with combined aggregates of continuous PSD can exhibit higher packing density, and thus higher workability given the cement content. In other words, an optimized PSD can enhance the packing density of the system, thus improving workability of the RCC, given the increase in excess paste film thickness around aggregate particles. The particle packing density can be affected by the aggregate characteristics, including the size, volume, shape, texture, and PSD of the aggregate constituents as well as the sand-to-total aggregate ratio (S/A). Regardless

of aggregate type, the packing density of a given aggregate combination can increase with the increase in S/A, up to a certain threshold value. Beyond such threshold, the packing density decreases with further increase in fine aggregate content. This can decrease in packing density due to the loosening and wall effects, which can push away the large particles and eventually result in voids among particles (Khayat and Mehdipour 2017).

The increase in aggregate volume and S/A generally can increase the water content required to reach given workability. The use of a higher fine aggregate proportion increases the surface area, which necessitates a higher paste volume needed to coat the particles.

In terms of segregation resistance of RCC, crushed aggregates are preferred since the interlocking friction among the particles can reduce the risk of aggregate separation. Another important factor influencing segregation resistance of aggregate combinations is the percentage retained on each sieve. The general rule is that the amount of retained aggregate on each sieve should not vary significantly from that of the next one. This can ensure that all sizes of aggregates are available in the mixture, which reduces the risk of segregation.

2.2.2. Mechanical properties

RCC is a multiple-phase material with aggregate, cement paste, and an interfacial transition zone between the paste and aggregate. Generally, the mechanical behavior of RCC is similar to that of ordinary concrete. Some researchers have reported that the mechanical properties of RCC, including compressive strength, flexural strength, shear strength, and toughness can be greater than those of ordinary concrete (Piarc 1993; Tayabgi and Okamoto 1987).

As mentioned earlier, given the limited binder content in RCC, the optimization of the solid skeleton through minimizing the void ratio of solid particles is crucial. As stated earlier, the

Missouri Standard Specifications for Highway Construction requires that RCC prepared according to ASTM C 1176 or ASTM C 1435 to have a minimum compressive strength of 3,500 psi (24 MPa) at 28 days. Highly dense graded aggregates of RCC mixtures can help achieve high compressive strength. RCC mixtures with optimized PSD can reach a relatively dense structure under adequate vibration energy. There often exists an optimal coarse aggregates volume, at which the highest compressive strength can be obtained. However, increasing the coarse aggregate beyond this threshold can decrease compressive strength (Cetin and Carrasquillo 1998).

Flexural and tensile strengths are important parameters for RCC. The use of steel or polypropylene fibers can enhance ductility, greater flexural and tensile strengths, as well as to reduce cracks and achieve a designed thickness of pavement (Madhkhan et al. 2015). Kagaya et al. (2001) found that the toughness and flexural strength of RCC pavements with fiber were higher than those of RCC without any fiber. Angelakopoulos et al. (2009) reported that at a constant steel fiber volume, use of longer fibers with a length greater than 2 in. (50 mm) can improve the load-deflection behavior of RCC. This is because longer fibers are more efficient in arresting and bridging cracks. Madhkhan et al. (2011 and 2012) reported that the use of steel fibers alone did not exert a considerable effect on enhancing the flexural strength; however, the flexural strength increased when the concrete was proportioned with high pozzolan content.

The quality of fiber-matrix interface plays a significant role in improving tensile strength and toughness of RCC. The use of pozzolans, such as silica fume, fly ash, or slag cement can improve bond properties between the fiber and the cement paste matrix due to the filler and pozzolanic effects, thus enhancing strength and ductility of RCC. In addition, the aggregate skeleton of RCC can provide friction and/or anchorage action during fiber pullout and/or fracture

processes to contribute to the strength and toughness. Therefore, optimized PSD of the aggregate system can ensure denser particles contact and better stress transfer efficiency from the matrix to the reinforcing fibers, thus enhancing the mechanical properties of RCC.

2.3. Durability of RCC in cold climate

(1) Freeze-thaw resistance

Field studies of RCC used in dam and pavement construction have indicated that RCC can develop satisfactory freeze-thaw resistance in harsh weather conditions (Liu, 1991). Investigation carried out in the United States and Canada indicated that RCC mixtures, whether air-entrained or not, have performed well for more than three decades (Piggott, 1999). Non-air entrained RCC pavements can provide adequate frost durability in mixtures made with sufficient cement content and sound aggregates and subjected to proper mixing, compaction, and curing. This is due to relatively impermeable microstructure, thus minimizing the path for water to critically saturate the concrete.

Previous investigations of the freeze-thaw resistance of RCC show conflicting findings, as summarized in Table 2.3. For example, Ghafoori and Cai (1998) indicated that the durability factor after 300 cycles of freezing and thawing of non-air entrained RCC made with 364 lb/yd^3 (216 kg/m^3) of cementitious materials was as high as 90% with a mass loss lower than 2%. This agrees well with the results reported by Vahedifard et al. (2010) who found modulus durability factor of 80% and a mass loss less than 1.5% for RCC made with 485 lb/yd^3 (288 kg/m^3) of cementitious materials. However, Delatte and Storey (2005) reported a mass loss greater than 7% for non-air-entrained RCC made with 440 - 550 lb/yd^3 (261 - 326 kg/m^3) of cementitious materials. Mardani et al. (2013) reported a durability factor less than 70% after 300 cycles for

non-air-entrained RCC made with 421 lb/yd^3 (250 kg/m^3) of binder (cement and fly ash) at w/cm range of 0.39 to 0.4.

Table 2.3. Summary of freeze-thaw resistance of RCC mixtures

	Cementitious materials content, lb/yd^3 (kg/m^3)	w/cm	Air-entrained or not	Mass loss after 300 cycles	Durbility factor after 300 cycles
Ghafoori and Cai (1998)	364 (216), 485 (288), and 607 (360)	0.45 - 0.89	No	< 2%	90%, 94%, and 97%
Delatte and Storey (2005)	550 (326), 489 (290), and 440 (261)	0.4, 0.45, and 0.5	No	> 7%	-
Vahedifard et al. (2010)	401 (238) and 460 (273)	0.41 and 0.46	No	< 1.5%	80%
Hazaree et al. (2011)	169 - 421 (100 - 250)	0.5 - 1.27	No	-	< 60%
	506 - 758 (300 - 450)	0.27 - 0.41	No	-	60% - 80%
	590 - 758 (350 - 450)	0.26-0.34	Yes	-	90%
Mardani et al. (2013)	421 (250)	0.39-0.47	No	< 2%	< 70%

The incorporation of AEA is effective in creating proper air-void systems in conventional concrete to enhance frost durability. Low w/cm and good compaction can provide RCC mixture with a minimum amount of freezable water in the capillaries, thus resulting in low water permeability. RCC pavement cannot be damaged by freeze-thaw cycles if the material is not critically saturated (Rollings, 1988).

(2) Deicing salt scaling

Generally, concrete specimens with higher density can develop greater resistance to deicing salt scaling. RCC appears to be more susceptible to deicing salt-scaling than conventional portland cement concrete mixtures of the same compressive strength (PCA 1994). Compressive strength alone is not a reliable indicator of potential scaling of RCC. For example,

non-air-entrained RCC with a 28-d compressive strength of 7400 to 8500 psi (51 to 59 MPa) showed moderate to severe scaling after 35 freeze-thaw cycles in the presence of deicing salt. Air-entrained RCC with a 28-d compressive strength of 4600 to 7700 psi (32 to 53 MPa) showed slight to moderate scaling when subjected to 80 freeze-thaw cycles (PCA 1994).

A series of scaling tests carried out on specimens taken from field projects indicates that the binder type can play a significant role in deicing salt scaling resistance. SCM, especially silica fume, can be used to improve RCC scaling resistance.

(3) Abrasion resistance

RCC used as paving materials must possess adequate abrasion resistance for vehicle types and traffic. It is often assumed that concrete abrasion resistance is guaranteed when compressive strength is high. However, this is not always correct because abrasion resistance is a surface property that depends mainly on surface layer characteristics (Kreijger 1984). The concrete mixture proportioning, surface finishing quality, curing regime, and construction technique can have a significant effect on the abrasion resistance of RCC. Standard abrasion resistance testing methods, including ASTM C418, ASTM C 779, and ASTM C 994, are often used to assess the abrasion resistance of concrete.

Nanni (1989) investigated the abrasion resistance of RCC according to ASTM C 779, Procedure C. It was found that the top surface of field-cut samples was much better than that of the saw-cut side if testing was conducted under air-dry conditions. This difference was significantly reduced under wet conditions. For laboratory specimens, the quality of the surface in contact with the mold was substantially lower than that of field-cut specimens. The addition of steel or synthetic fiber was found not to affect abrasion resistance of the surface layer subjected

to action of the abrasive tool (Nanni 1989). However, a clear benefit was demonstrated in the case of fiber-reinforced RCC pavements subjected to vehicular traffic.

3. EXPERIMENTAL PROGRAM

3.1. Materials

The materials selected for preparing RCC mixtures, including the cementitious materials, aggregates, and chemical admixtures are shown below.

3.1.1. Cementitious materials

A Type I portland cement was used for the RCC mixtures. A Class C fly ash (FAC) was also used in a binary system to develop different binder compositions in selected mixtures. Figure 3.1 shows the PSD and physical and chemical characteristics of the cementitious materials that are given in Table 3.1.

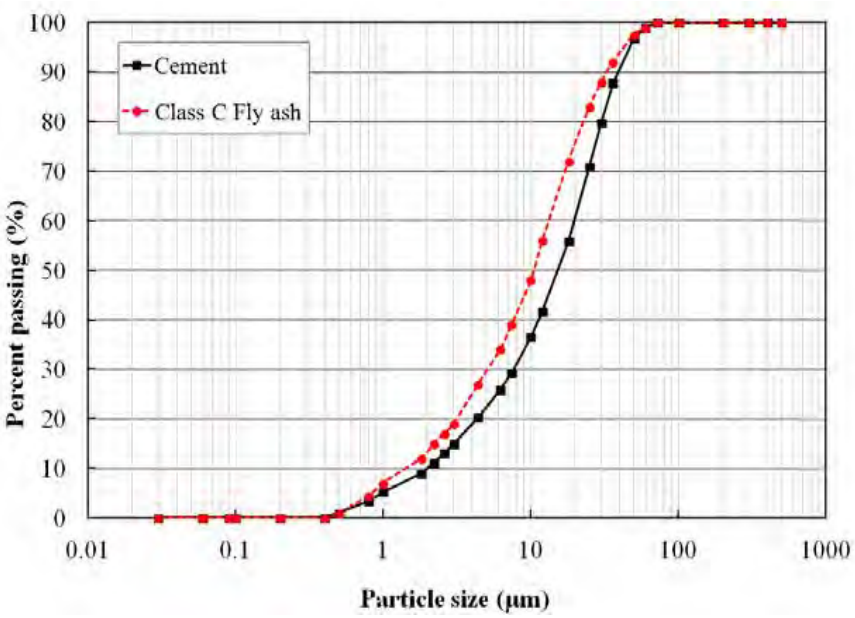

Figure 3.1. PSD of cementitious materials

3.1.2. Chemical admixtures

A commercially available AEA was used to entrain air in the RCC mixtures. The AEA is a liquid solution with a specific gravity of 1.05 and a solid content of 12%.

Table 3.1. Physical and chemical characteristics of cementitious materials

Characteristic	OPC	FAC
SiO_2 (%)	19.8	36.5
Al_2O_3 (%)	4.5	24.8
Fe_2O_3 (%)	3.2	5.2
CaO (%)	64.2	28.1
MgO (%)	2.7	5
SO_3 (%)	3.4	2.5
$CaCO_3$ (%)	3.3	–
Blaine surface area (m^2/kg)	390	498
Density (g/cm^3)	3.14	2.71
LOI (%)	1.6	0.5

3.1.3. Aggregates

As mentioned earlier, the selection of proper aggregate combination with optimized PSD is necessary to achieve high packing density, which can enhance the performance of RCC. Such an optimization, however, depends on the physical properties of the aggregate that vary with the type of aggregate. The aggregate used in this study was selected in a way to cover a wide range of materials available in Missouri. The aggregate selection procedure is briefly described in Section 3.2.1. The preliminary results conducted on selected aggregates are discussed in section 3.2.2.

3.2. Testing program

The methodology to develop and optimize RCC mixtures with optimized aggregate combinations and air-void system is described in the following section. The approach consisted of designing optimized aggregate combination with maximum possible packing density, optimization of non-air-entrained RCC with high packing density, adequate workability, and strength, as well as optimization of air-entrained RCC with proper adequate air-void system and high durability characteristics.

3.2.1. Subtask I - Selection and optimization of aggregate combination

(1) Aggregate selection

Various aggregate producers are available in Missouri for different applications from different quarries. About 40 aggregate types sampled from various quarries were examined. Aggregate characteristics, including PSD, specific gravity, bulk density, and absorption were collected. Figure 3.2 shows the locations of various aggregate quarries visited in this investigation to study the aggregate characteristics.

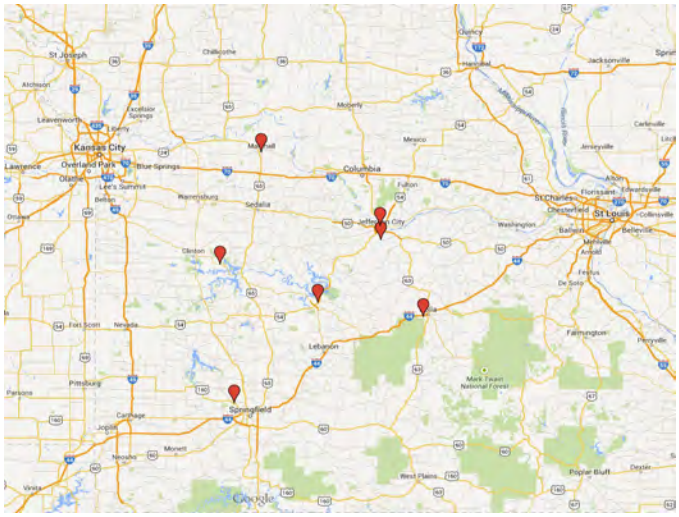

Figure 3.2. Locations of aggregate quarries visited in this investigation (Mehdipour, 2017)

Fine, intermediate, and coarse aggregates were investigated. PSD of each examined aggregate is summarized in Figure 3.3. This figure shows the wide range of aggregate examined in this investigation. The maximum nominal size of coarse aggregate was limited to 1 in. (2.5 mm). Both crushed and rounded aggregates were considered. Photographs of 17 selected aggregates employed for preliminary evaluation are shown in Figure 3.4.

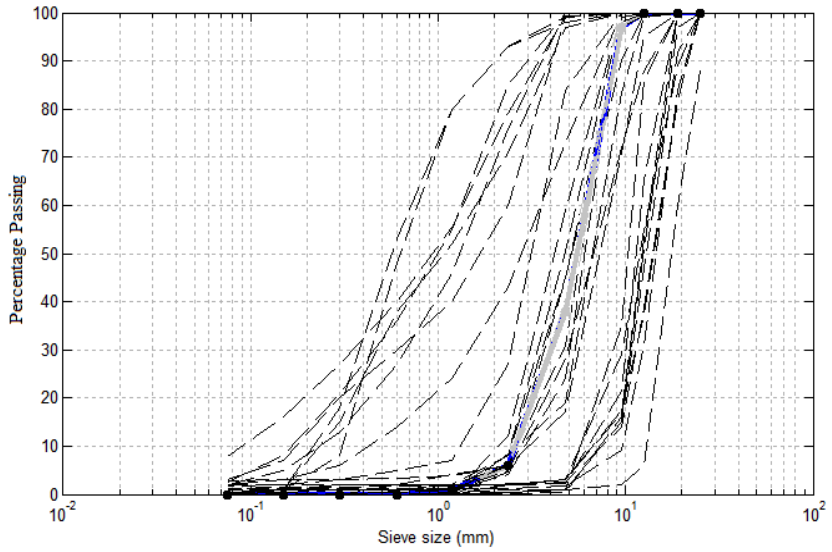

Figure 3.3. PSD of examined aggregates

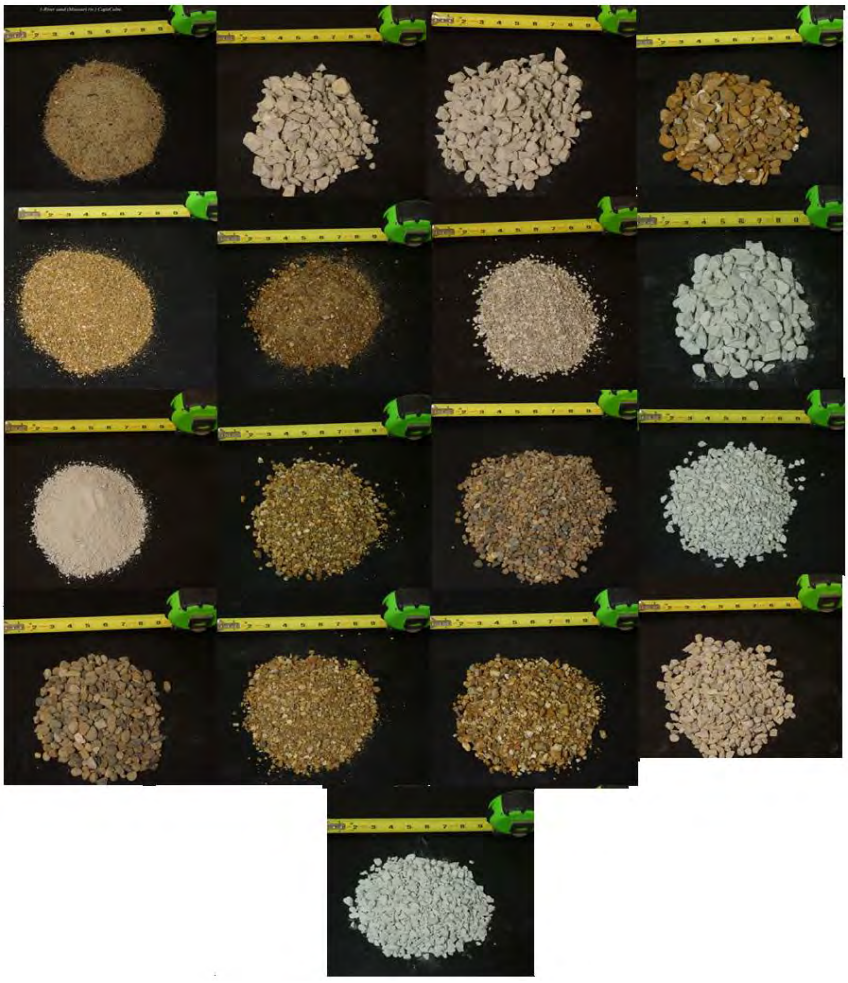

Figure 3.4. Photos of sampled aggregates (Mehdipour, 2017)

A numerical investigation was performed on various binary and ternary blends of aggregates to select the aggregate combinations. Aggregates were ranked based on the residual error defined as the minimum deviation of aggregate combinations from the target grading. The target grading was considered to be the modified Andreasen and Andersen grading with the maximum and minimum particle sizes of 3/4 in. (19.1 mm) and 0.0008 in. (20 micron), respectively. In addition to numerical analysis ranking, aggregates were selected to have both crushed and rounded aggregate in the final experimental step. Characteristics of selected aggregates in this step are shown in Table 3.2.

(2) Determination of packing density of individual aggregate

Packing densities of aggregates with various physical properties were determined using the ICT. The packing densities of aggregates were also obtained in loose and rodded situation for comparison. The obtained aggregate packing density of individual aggregate is summarized in Table 3.3. From the results, the packing densities of aggregates were shown to vary with size, shape, surface texture, and angularity of aggregate. The packing densities of the investigated fine, intermediate, and coarse aggregates vary between 0.58 - 0.72, 0.60 - 0.68, and 0.59 - 0.61, respectively. The packing density data is required for numerical modeling of aggregate packing which will be performed in the next subtask of this project.

Table 3.2. Aggregates selected for further investigation (Mehdipour, 2017)

Aggregate size	Name	Shape
Fine	River sand (1)	Rounded
	River sand (2)	Rounded
	Crushed sand (1)	Crushed
	Crushed sand (2)	Crushed
	Crushed sand (3)	Crushed
Intermediate	5/16" aggregate	Rounded
	3/8" aggregate (1)	Crushed
	3/8" aggregate (2)	Crushed
	3/8" aggregate (3)	Crushed
	7/16" aggregate	Rounded
	1/2" aggregate (1)	Crushed
	1/2" aggregate (2)	Crushed
	1/2" aggregate (3)	Crushed
Coarse	3/4" aggregate	Crushed
	1" aggregate	Rounded
	1" aggregate (1)	Crushed
	1" aggregate (2)	Crushed

Table 3.3. Results of packing density of selected aggregates (Mehdipour, 2017)

Aggregate size	Name	Relative density	Bulk density (ICT*) (lb./ft^3)	Bulk density (loose) (lb./ft^3)	Bulk density (rodding) (lb./ft^3)	Packing density (ICT*)	Packing density (loose)	Packing density (rodding)
Fine	River sand (1)	2510	1838	1671	1800	0.73	0.67	0.72
		2510	1829	1682	1797	0.73	0.67	0.72
	River sand (2)	2517	1810	1729	1792	0.72	0.69	0.71
		2517	1821	1729	1794	0.72	0.69	0.71
	Crushed sand (1)	2480	1619	1454	1548	0.65	0.59	0.62
		2480	1613	1453	1549	0.65	0.59	0.62
	Crushed sand (2)	2582	1536	1353	1496	0.59	0.52	0.58
		2582	1533	1353	1490	0.59	0.52	0.58
	Crushed sand (3)	2606	1934	1670	1751	0.74	0.64	0.67
		2606	1872	1670	1768	0.72	0.64	0.68
Intermediate	5/16" aggregate	2590	1702	1608	1696	0.66	0.62	0.65
		2590	1693	1600	1694	0.65	0.62	0.65
	3/8" aggregate (1)	2450	1638	1546	1641	0.67	0.63	0.67
		2450	1663	1546	1665	0.68	0.63	0.68
	3/8" aggregate (2)	2430	1484	1350	1470	0.61	0.56	0.60
		2430	1485	1358	1472	0.61	0.56	0.61
	3/8" aggregate (3)	2450	1516	1360	1473	0.62	0.56	0.60
		2450	1520	1363	1473	0.62	0.56	0.60
	7/16" aggregate	2590	1660	1600	1648	0.64	0.62	0.64
		2590	1659	1565	1656	0.64	0.60	0.64
	1/2" aggregate (1)	2430	1535	1420	1500	0.63	0.58	0.62
		2430	1538	1410	1510	0.63	0.58	0.62
	1/2" aggregate (2)	2730	1631	1500	1614	0.60	0.55	0.59
		2730	1653	1503	1630	0.61	0.55	0.60
	1/2" aggregate (3)	2462	1581	1450	1561	0.64	0.59	0.63
		2462	1569	1454	1578	0.64	0.59	0.64
Coarse	3/4" aggregate	2570	1507	1410	1527	0.59	0.55	0.59
		2570	1492	1427	1534	0.58	0.56	0.60
	1" aggregate	2450	1498	1426	1493	0.61	0.58	0.61
		2450	1472	1426	1505	0.60	0.58	0.61
	1" aggregate (1)	2572	1514	1457	1534	0.59	0.57	0.60
		2572	1515	1470	1533	0.59	0.57	0.60
	1" aggregate (2)	2689	1648	1471	1590	0.61	0.55	0.59
		2689	1640	1470	1578	0.61	0.55	0.59

** Compacted with ICT gyratory compactor*

3.2.2. Subtask II - Optimization of aggregate combination

This subtask was to optimize the aggregate proportions to achieve the maximum packing density of combinations of fine, intermediate, and coarse aggregates. Given various aggregate combinations, the preliminary selection of optimum aggregate combination was carried out using existing theoretical packing density. The selected aggregate combinations (sand, intermediate, and coarse aggregates) with relatively high packing density were experimentally validated. In this phase, measured packing densities were compared with those estimated from theoretical packing density models. The selected aggregate combinations were proportioned with various sand-to-total aggregate ratios to optimize the proportioning for a given aggregate combination. In order to determine the optimum proportioning of the aggregate blend, the statistical mixture design (SMD) method was utilized. SMD method provides an efficient tool for determining the predicted model as well as for optimizing the mixture proportion. In this method, the main principle is that the sum of all constituents for a given mixture is equal to 1. In general, assuming that the mixture consists of n constituents at which x represents the proportion of the i^{th} constituent in the mixture, the sum of the material constituents is expressed as follows:

$$0 \le x_i \le 1 \qquad i = 1, 2, ..., n \qquad \sum_{i=1}^{n} x_i = 1 \qquad \text{(Eq. 3.1)}$$

This method can be effectively employed to determine the optimum proportions of blended aggregates to achieve the possible maximum packing density. Various aggregate proportions used for SMD is given in Table 3.4. The results of the packing density of blended aggregates are used as input to derive the prediction model for packing density response. The derivation of numerical model enables the determination of optimal aggregate proportion corresponding to the achievable maximum packing density.

Table 3.4. Proportions of aggregate combinations used for SMD

Mix #	Aggregate ratio (mass)		
	Sand	Intermediate aggregate	Coarse aggregate
R1	40%	20%	40%
R2	40%	10%	50%
R3	40%	30%	30%
R4	50%	10%	40%
R5	50%	20%	30%
R6	60%	10%	30%
R7	30%	20%	50%
R8	30%	30%	40%
R9	60%	0%	40%
R10	60%	20%	20%
R11	50%	30%	20%
R12	44%	18%	38%
R13	20%	20%	60%
R14	20%	30%	50%
R15	30%	10%	60%
R16	30%	40%	30%
R17	40%	15%	45%

Finally, the selected aggregate combinations were ranked based on the residual error defined as the minimum deviation of aggregate combinations from the target grading. The target grading was considered to be the modified Andreasen and Andersen grading with the maximum and minimum particle size of 0.75 in. (19 mm) and 0.0008 in. (20 micron), respectively.

The packing density results are shown in ternary diagrams (Figure 3.5). Given different aggregate combinations and proportions, the packing density of the aggregate combinations varied from 0.63 to 0.82. Regardless of aggregate type, the packing density of blended aggregate increased with the increase in fine-to-total aggregate ratio up to a certain threshold value, beyond which the maximum packing density decreased with further increase in fine aggregate replacement. This can be due to the loosening and wall effect, which can push the large particles away, thus leading to lower packing density. Apparently, there exists an optimum value of

aggregate proportions, corresponding to maximum packing density, which can significantly reduce the void volume between particles. The optimal aggregate blend was found to consist of 40% sand, 20% intermediate aggregate, and 40% coarse aggregate, which has a packing density of more than 0.8. This lowers the paste volume required to fill the voids between the granular skeleton. The effect of the aggregate gradation on properties of RCC was explored further.

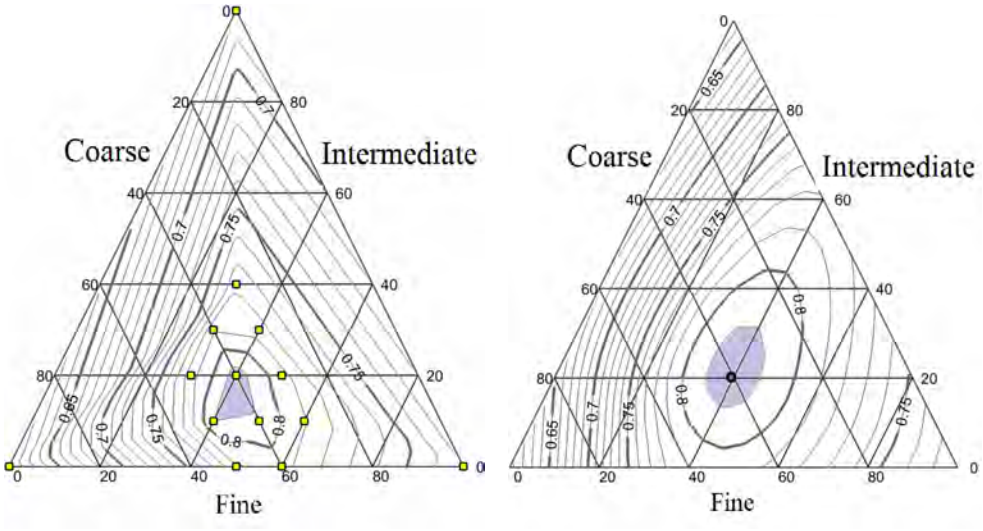

(a) Packing density (b) Toufar packing density model

Figure 3.5. Ternary diagrams of aggregate packing density

3.2.3. Subtask III - Optimization of non-air-entrained RCC made with different aggregate combinations

This subtask focused on evaluating the effect of mixture proportions on workability, surface electrical resistivity, density, and compressive strength of non-air-entrained RCC mixtures made with different aggregate combinations. In total, 17 mixtures were evaluated.

3.2.4. Subtask IV - Optimization of air-entrained RCC

This subtask developed production techniques to adjust the amount of entrained air in RCC. The degree of consolidation and uniformity of the air-void system are of prime importance for frost durability and were investigated in this task. It aimed at evaluating the several

parameters on compressive strength, permeable void ratio, electrical resistivity, freeze-thaw resistance, and deicing salt-scaling resistance of air-entrained RCC mixtures. Eleven mixtures were initially developed to examine strength, surface electrical resistivity, and air-void system, four mixtures were then investigated for durability. The testing matrix of this subtask is presented in Table 3.5. The investigated parameters in this subtask include the following:

(1) AEA dosage: medium (AM), high (AH), and very high (AV);

(2) Workability level: Vebe Time 90 - 60 s (WL), 60 - 30 s (WM), and 30 - 15 s (WH). The workability level was adjusted by changing the water-to-solid ratio of the mixtures.

(3) Binder volume: low (BL), medium, and high (BH);

(4) Mixer type: Omni mixer (MO), drum mixer, and Eirich high shear rate mixer (MH);

(5) Compaction techniques: vibrating hammer (CH), Vebe vibrating table (CV), and ICT.

Table 3.5. Testing matrix for Subtask IV

No.	Binder volume			Vebe Time (Workability)			Mixer type			Compaction			AEA dosage		
	Low	Medium	High	Low	Medium	High	Omni	Drum	Eirich	Vebe	Hammer	ICT	Medium	High	Very high
AEA dosage level		x			x			x				x	x		
		x			x			x				x		x	
		x			x			x				x			x
Binder volume	x				x			x				x		x	
		x			x			x				x		x	
			x		x			x				x		x	
Workability		x		x				x				x		x	
		x			x			x				x		x	
		x				x		x				x		x	
Mixer type		x			x		x					x		x	
		x			x			x				x		x	
		x			x				x			x		x	
Compaction type		x			x			x		x				x	
		x			x			x			x			x	
		x			x			x				x		x	

3.3. Mixing and testing methods

3.3.1. RCC mixing procedure

Aggregates were maintained at 73 °F (23 °C) for at least 24 hours before mixing. Separate aggregates were tested for moisture correction before mixing. The aggregates were loaded into the mixer along with two-thirds of the mixing water. Three types of mixer, including an ordinary drum mixer (capacity of 0.13 yd^3) [100 L], a Omni mixer with central shaft (capacity of 0.026 yd^3) [20 L], and an Eirich high shear mixer (capacity of 0.20 yd^3) [150 L], were used, as shown in Figure 3.6. All aggregates and part of the water were mixed for three minutes to allow the aggregates to approach the saturated surface dry (SSD) condition. The cement and remaining water were then added and mixed for three minutes. The same mixing procedure was used for the three mixers.

Three compaction technologies, including vibrating hammer, ICT gyratory compactor, and Vebe vibrating table, were employed (Figure 3.7). For mixtures with high and medium workability levels, surface quality as shown in Figure 3.8 was secured.

(a) Omni mixer (b) Drum mixer (c) Eirich high shear mixer

Figure 3.6. Three mixer types used for preparing RCC

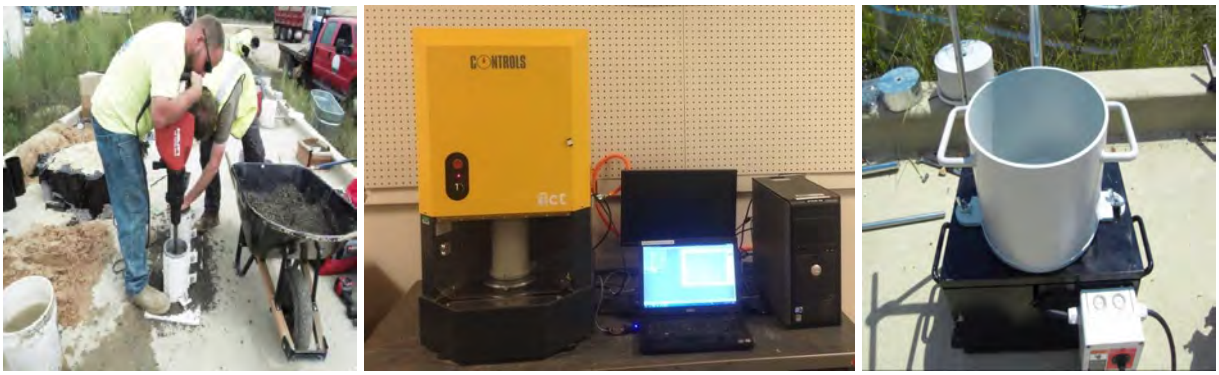

(a) Vibrating hammer (b) ICT gyratory compactor (ICT-100R) (c) Vebe vibrating table

Figure 3.7. Three different compaction techniques used for preparing RCC

3.3.2. Testing methods for RCC mixtures

RCC mixtures were prepared to evaluate the effect of different aggregate combinations and air-void systems on performance, including workability (Vebe time), segregation index, density, electrical surface resistivity, compressive and splitting strengths, modulus of elasticity, and durability characteristics. The testing methods used are presented below.

(1) Workability (Vebe time)

RCC workability was conducted using a Vebe apparatus according to ASTM C1170. Immediately after mixing, the fresh properties of the mixtures were investigated. The dimensions of the cylindrical mold were measured and the interior of the mold was dampened with a wet cloth. The mass of the cylindrical mold was measured and 29.8 lb (13.5 kg) of concrete was added into the mold using a square ended scoop. The mold was fixed on the vibrating table by tightening the wingnuts. The shaft with surcharge mass weighing 50.0 lb (22.7 kg) and a plastic plate attached to its base was lowered onto the top of the concrete and was then vibrated. The vibration was continued until the mortar ring formed completely around the plastic plate and the time was recorded as the Vebe consistency time. In the absence of mortar ring formation within 60 seconds from the start of vibration, the vibrating table was turned off and the Vebe

consistency time was recorded to be greater than 60 seconds. Figure 3.8 compares concrete surface of RCC with high and medium workability levels.

Figure 3.8. Concrete surface after Vebe testing for (a) dry RCC with low workability level (Vebe time ≥ 90 s; (b) RCC with medium workability level (Vebe time = 45 s) (Khayat and Libre, 2014)

(2) Segregation index

An attempt to create a new test method to evaluate the segregation risk of fresh RCC was performed. In this procedure, a representative sample of concrete (7 - 8 lb) [3.2 - 3.6 kg] was rotated for 10 revolutions in a drum with an inclination of 30 degrees to simulate concrete mixing and enable segregation to occur. Concrete sample was then dropped from a height of approximately 2 ft (0.6 m) over a flat surface in order to induce some material separation (i.e., segregation). The concrete was divided into inner and outer parts (almost equal in portions). Both samples were weighed and then washed over sieve No. 4 (0.19 in.) [4.8 mm] to remove all of the mortar and fine particles. The weight of coarse aggregate, including the pea gravel, retained over the No. 4 sieve (0.19 in.) [4.8 mm] were measured, and the segregation index was calculated from the following equation:

$$SI = \sqrt{(R_i - R_t)^2 - (R_e - R_t)^2} \quad \text{(Eq. 3.2)}$$

where, $R = (w_{CA}/w_C)$; w_{CA} is the weight of coarse aggregate; w_C is the weight of concrete; R_i and R_e are coarse-to-concrete weight ratios of the inner and outer parts, respectively; and R_t is the coarse-to-concrete weight ratio of the whole concrete sample.

An SI = 0 means that the concrete is completely homogeneous. A higher value of SI reflects a greater variation of coarse aggregate in the inner and outer parts of concrete sample, thus indicating a greater risk of aggregate separation and segregation of the RCC mixture.

(3) Density of hardened concrete

The density of hardened concrete in saturated-surface dry (SSD) condition was measured according to ASTM C642 in order to find the variation of density in different samples for the same mixture.

(4) Surface resistivity

Surface electrical resistivity of RCC specimens was measured in accordance with AASHTO T95. The surface resistivity test method consists of measuring the resistivity of 4 × 8 in. (102 × 203 mm) cores or cylinders using a 4-pin Wenner probe array, as illustrated in Figure 3.9. An AC potential difference is applied in the outer pins of the Wenner array generating current flow in the concrete. The potential difference generated by this current is measured using the two inner probes. The current used and potential obtained along with the area affected are used to calculate the resistivity of the concrete. The surface resistivity of concrete specimens at 7, 14, 21, and 28 days after sampling were measured. Table 3.6 summarizes the relation between the surface resistivity and the risk of corrosion in concrete.

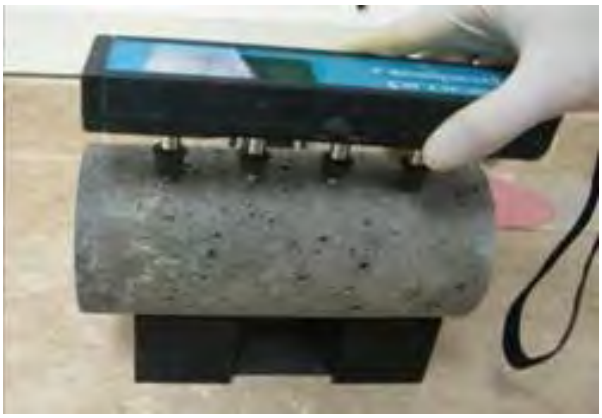

Figure 3.9. Testing apparatus for surface electrical resistivity of RCC

Table 3.6. Relation between surface resistivity and risk of corrosion in concrete

Chloride ion penetrability	Surface resistivity test (kΩ.cm) [4 × 8 in. (102 × 203 mm)]
High	< 12
Moderate	12-21
Low	21 - 37
Very low	37 - 254
Negligible	> 254

(5) Compressive strength

The 7 and 28-d compressive strengths of cylinders measuring 4 × 8 in. (102 × 203 mm) were determined according to ASTM C39. The cylinders were cured in lime-saturated water at a controlled temperature of 69.8 ± 3.6 °F (21 ± 2 °C) until testing age. Average values of three specimens were reported. The values of coefficient of variation (COV) of compressive strength results were set to be lower than 5%.

(6) Splitting tensile strength

The standard procedure of splitting tensile strength is described in ASTM C496. The setup used for measuring the splitting tensile strength is shown in Figure 3.10. Compressive loads (P) are applied on the top and bottom of the specimens measuring 6 × 12 in. (152 × 305 mm) cylinders, where two strips of plywood are placed to distribute tensile stress along the

vertical axis of the specimens. The load at failure is recorded as the peak load, and the tensile strength is calculated using the following equation:

$$f_t = \frac{P}{\pi DL} \quad \text{(Eq. 3.3)}$$

where P is the peak load (N); L is the length of the specimen (m); D is the diameter of the specimen (m).

Figure 3.10. Splitting tensile test setup

(7) Modulus of elasticity

The modulus of elasticity was determined according to ASTM C469 using an MTS machine (Figure 3.11). For each testing age, three cylindrical specimens measuring 4 × 8 in. (102 × 203 mm) were used for determining the modulus of elasticity. The end surfaces of specimens were ground to ensure uniform load distribution.

(8) Spacing factor

Specimens measuring 4 × 1 in. (102 × 25 mm) cut from larger cylindrical specimens were prepared to determine the air-void system according to ASTM C 457. Two specimens for each mixture were tested.

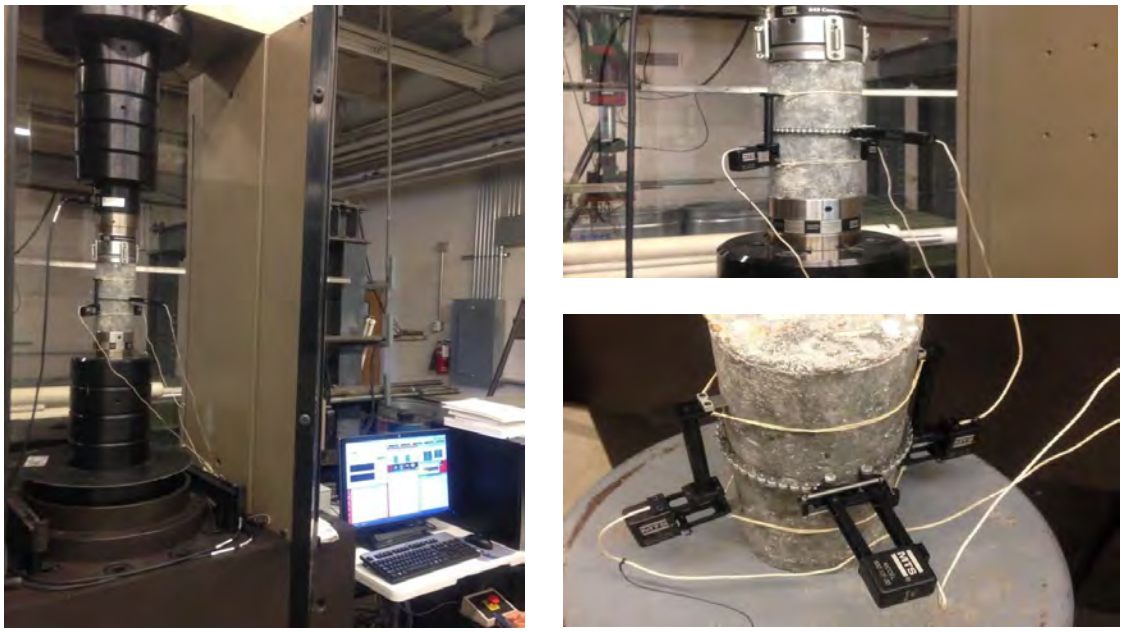

Figure 3.11. Test setup for modulus of elasticity measurement

(9) Freeze-thaw resistance

The freeze-thaw resistance of RCC samples was evaluated in accordance with ASTM C666, Procedure A. The test procedure consists of subjecting concrete specimens to 300 cycles of rapid freezing and thawing in water at temperatures varying between 41 to -0.4 °F (5 to -18 °C). The specimens are placed in metal containers and surrounded by approximately 0.2 in. (5 mm) of clean water in a specified chamber, as illustrated in Figure 3.12. Freezing is generated with a cooling plate at the bottom of the apparatus, whereas thawing is produced by heating elements placed between the containers. The change in mass and durability factor were determined. The dynamic modulus of elasticity of concrete specimens subjected to freeze-thaw cycles is measured, using the testing apparatus shown in Figure 3.13. Drop in dynamic modulus of elasticity is an indicator of internal cracking damage caused by freeze-thaw cycles. Figure 3.14 shows RCC specimens before the freeze-thaw test.

Figure 3.12. Freeze-thaw chamber according to ASTM C666, Procedure A

Figure 3.13. Testing apparatus for dynamic modulus of elasticity

Figure 3.14. RCC specimens before the freeze-thaw test

(10) Deicing salt-scaling resistance

Deicing salt scaling tests were carried out using three slabs measuring 11 × 10 × 3 in. (279 × 254 × 72 mm) for each RCC mixture in accordance to ASTM C672. The specimens were cured in lime-saturated water until age of 28 days. During this test, the surface of concrete was covered with approximately 6 mm of with 4% sodium chloride solution i.e., 0.14 oz. (4 g) of NaCl for each (3.4 fl. oz.) [100 ml] of water). The specimens were subjected to 50 freezing and thawing cycles by alternately placing them in a freezing environment (-0.08 ± 3.02 °F) [-17.8 ± 1.7 °C] and a thawing environment (73.4 ± 3.1 °F) [23.0 ± 1.7 °C]. The chamber used is shown in Figure 3.15. At the end of each series of 5 cycles, the salt solution was renewed, and the scaling residues were recuperated, dried, and weighed. The extent of surface scaling was assessed visually according to Table 3.7. The visual rating of zero means no scaling for concrete surfaces and five for severe scaling with coarse aggregates visible over the entire surface. The mass of scaled materials was also determined by removing the scaled materials at regular intervals using low-pressure water jetting and drying the scaled materials in an oven.

Figure 3.15. Chamber used for deicing salt-scaling resistance test

Table 3.7. Visual rating of the surface after certain salt-scaling cycles

Rating	Condition of surface
0	No scaling
1	Very slight scaling(1/8 in. [3 mm] depth, max, no coarse aggregate visible
2	Slight to moderate scaling
3	Moderate scaling (some coarse aggregate visible)
4	Moderate to severe scaling
5	Severe scaling (coarse aggregate visible over entire surface)

(11) Permeable voids

Permeable voids of RCC specimens were determined in accordance with ASTM C642. The testing apparatus used in this investigation is shown in Figure 3.16. This test method determines the water absorption after immersion in water and after immersion in boiling water for five hours. The high temperature affects both the viscosity and the mobility of the water molecules, which may lead to the greater displacement of water within the pore structure of the hardened concrete. Samples were dried in an oven at a temperature of 230 ± 9 °F (110 ± 5 °C) until a constant mass (A) was obtained. The specimens were then immersed in water at approximately 70 °F (21 °C) for not less than 48 h to determine the saturated surface dried (SSD) mass (B). The specimens were then immersed in boiling water for five hours, and the SSD mass after boiling was determined (C). The apparent mass (D) of specimens was measured to determine the permeable void content. The absorption after immersion (m_1), absorption after immersion and boiling (m_2), and permeable void content (B_0) of the specimens are calculated using the following equations:

$$m_1 = [(B-A)/A] \times 100 \quad \text{(Eq. 3.4)}$$

$$m_2 = [(C-A)/A] \times 100 \quad \text{(Eq. 3.5)}$$

$$B_0 = (C-A)/(C-D) \times 100 \quad \text{(Eq. 3.6)}$$

Figure 3.16. Apparatus used for measuring permeable voids in concrete

4. TEST RESULTS AND DISCUSSION

The 17 aggregate combinations of different sizes, shapes, and proportions were used to prepare non-air-entrained RCC mixtures with a fixed w/cm of 0.4. The effect of aggregate combination on Vebe time, segregation index, density, surface electrical resistivity, and compressive strength were investigated.

The optimized RCC mixture with adequate workability and high strength was then selected to incorporate an AEA for air entrainment. The effect of AEA dosage, workability level, binder volume, mixer type, and compaction energy on the workability, surface electrical resistivity, compressive strength, frost resistance, and deicing salt scaling resistance of the air-entrained RCC mixtures was then evaluated.

4.1. Task 2 – Optimization of non-air-entrained RCC mixtures with different aggregate combinations

4.1.1. Mixture proportions

The mixture proportions of the 17 non-air-entrained RCC mixtures proportioned with different aggregates sizes, types, and combinations are presented in Table 4.1. The cement content and water-to-cement ratio (w/c) were fixed around 520 lb/yd^3 (309 kg/m^3) and 0.40, respectively, which are common in producing RCC. Moisture corrections were made to the batch water before mixing. No chemical admixtures were used in these RCC mixtures.

Table 4.1. Mixture proportions of non-air-entrained RCC mixtures made with different aggregate combinations

Mix #	Mixture proportions (lb/yd^3)					Mixture parameter	
	Sand	Intermediate aggregate	Coarse aggregate	Cement	Water	w/c	w/solid
R1	1300	628	1327	520	227	0.40	5.5%
R2	1314	317	1677	526	211	0.40	5.5%
R3	1316	953	1008	526	209	0.40	5.5%
R4	1643	317	1342	526	211	0.40	5.5%
R5	1641	634	1005	525	217	0.40	5.7%
R6	1970	317	1006	526	210	0.40	5.5%
R7	986	634	1677	526	210	0.40	5.5%
R8	984	950	1340	525	217	0.41	5.7%
R9	1928	0	1312	514	207	0.40	5.5%
R10	1946	626	662	519	207	0.40	5.5%
R11	1627	942	664	521	207	0.40	5.5%
R12	1422	562	1254	517	207	0.40	5.5%
R13	644	622	1973	515	207	0.40	5.5%
R14	647	937	1652	518	207	0.40	5.5%
R15	963	310	1967	514	207	0.40	5.5%
R16	977	1258	998	521	207	0.40	5.5%
R17	1290	467	1482	516	207	0.40	5.5%

4.1.2. Fresh properties

The Vebe time and segregation index of the investigated mixtures are summarized in Table 4.2. As can be seen from Table 4.2, the Vebe time varied significantly with the aggregate combinations. Low Vebe time of 7 s and high Vebe time up to 120 s were observed. Increasing the sand content with the constant w/c increased the Vebe time (reduced workability). For example, with the sand content increase from 1300 to 1970 lb/yd^3 (771 to 1169 kg/m^3), the Vebe time increased from 14 to 64 s. This is due to an increase in the surface area of the aggregate, which requires more water to lubricate their surface in order to produce the same level of workability.

Table 4.2. Fresh properties of non-air-entrained RCC mixtures

Mix #	Aggregate ratio (weight)			Vebe time	Segregation index
	Sand	Intermediate aggregate	Coarse aggregate		
	%	%	%	(sec)	
R1	40%	20%	40%	14	N.A.
R2	40%	10%	50%	10	N.A.
R3	40%	30%	30%	30	3.1
R4	50%	10%	40%	36	6.0
R5	50%	20%	30%	22	8.3
R6	60%	10%	30%	64	N.A.
R7	30%	20%	50%	7	N.A.
R8	30%	30%	40%	17	1.0
R9	60%	0%	40%	78	6.6
R10	60%	20%	20%	70	10.4
R11	50%	30%	20%	19	4.6
R12	44%	18%	38%	30	7.1
R13	20%	20%	60%	120	1.5
R14	20%	30%	50%	57	0.6
R15	30%	10%	60%	40	8.8
R16	30%	40%	30%	30	0.6
R17	40%	15%	45%	44	2.7

Ternary diagrams shown in Figure 4.1 were developed to study the effect of different aggregate combinations on Vebe time and segregation index of RCC. The ternary diagram of the segregation index, Figure 4.1(b), reveals that the concrete mixtures with higher sand and intermediate aggregate contents had higher segregation index values of up to 8. In other words, the risk of segregation was increased by increasing the sand and intermediate aggregate content above a certain value.

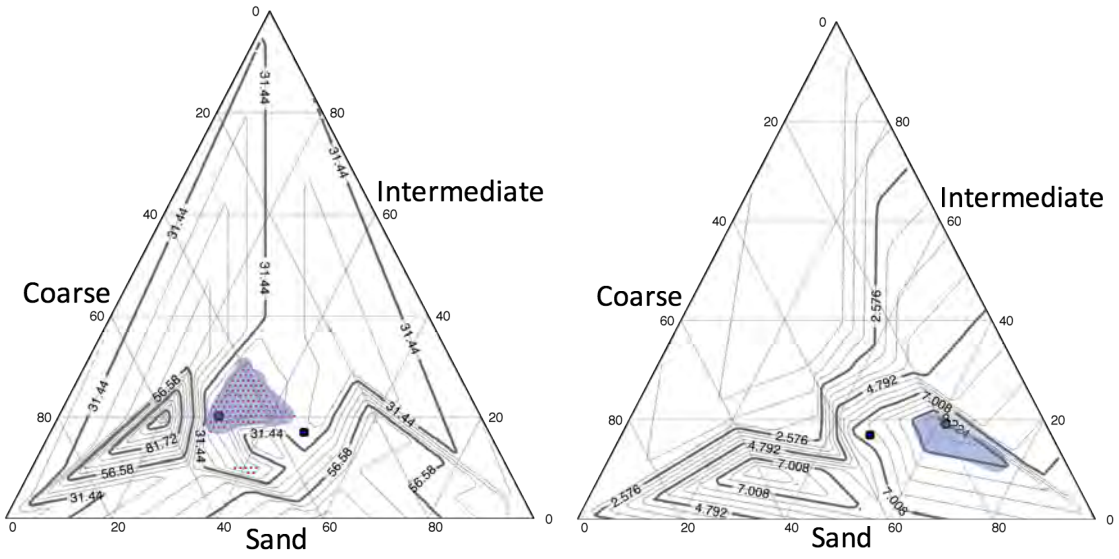

(a) Vebe time (b) Segregation index

Figure 4.1. Ternary diagrams of fresh properties of non-air-entrained RCC mixtures made with different aggregate combinations

4.1.3. Hardened properties

Figure 4.2 illustrates a contour of the variations of density of hardened non-air-entrained RCC mixtures proportioned with different shapes and replacement levels of aggregate. The density of hardened RCC ranged from 0.25 to 1.25, depending on the aggregate combination. The density increased with the increase in sand and intermediate aggregate contents above a certain value. RCC mixtures made with higher sand content of 60% to 80% were found to have greater densities around 0.75 - 1.25.

The results of the hardened properties are summarized in Table 4.3. Ternary diagrams of the corresponding results are illustrated in Figures 4.3 and 4.4.

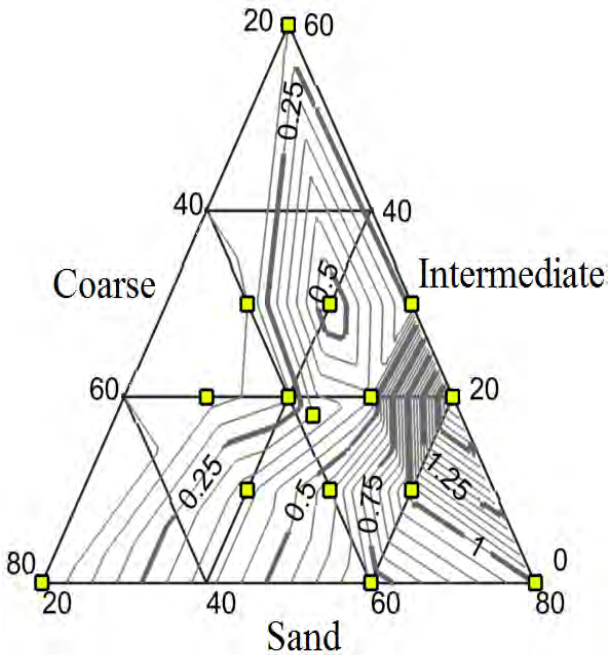

Figure 4.2. Variation of density in hardened non-air-entrained RCC mixtures

Table 4.3. Hardened properties of non-air-entrained RCC mixtures

Mix #	Aggregate ratio (weight)			Compressive strength		Surface resistivity			
	Sand	Intermediate aggregate	Coarse aggregate	7 d	28 d	7 d	14 d	21 d	28 d
	%	%	%	psi (MPa)	psi (MPa)	kΩ.cm	kΩ.cm	kΩ.cm	kΩ.cm
R1	40%	20%	40%	6850 (47.2)	7690 (53.0)	21	22	25	27
R2	40%	10%	50%	7280 (50.2)	7770 (53.6)	22	26	30	29
R3	40%	30%	30%	7470 (51.5)	7980 (55.0)	20	24	25	30
R4	50%	10%	40%	6820 (47.0)	7220 (49.8)	19	23	25	30
R5	50%	20%	30%	6310 (43.5)	7060 (48.7)	19	22	23	25
R6	60%	10%	30%	5120 (35.3)	4757 (32.8)	17	16	17	17
R7	30%	20%	50%	8220 (56.7)	8770 (60.5)	22	25	28	27
R8	30%	30%	40%	7610 (52.5)	8750 (60.3)	19	22	24	26
R9	60%	0%	40%	5630 (38.8)	6060 (41.4)	15	18	20	22
R10	60%	20%	20%	4470 (30.8)	4960 (34.2)	14	18	21	22
R11	50%	30%	20%	6670 (46.0)	7930 (54.7)	17	21	25	26
R12	44%	18%	38%	6210 (42.8)	7900 (53.8)	19	23	26	28
R13	20%	20%	60%	4860 (33.5)	3580 (24.7)	21	22	25	N.A.
R14	20%	30%	50%	5800 (40.0)	5010 (34.6)	19	22	25	N.A.
R15	30%	10%	60%	5150 (35.5)	8310 (57.3)	21	21	26	N.A.
R16	30%	40%	30%	6930 (47.8)	6790 (46.8)	19	23	N.A.	N.A.
R17	40%	15%	45%	6610 (45.6)	7830 (54.0)	25	24	N.A.	N.A.

As shown in Figure 4.3(a), the 7-d compressive strength indicates that the maximum compressive strength is achieved in RCC mixture with nearly maximum packing density; this corresponds to an aggregate combination with 40% sand, 20% intermediate aggregate, and 40% coarse aggregate. When greater coarse aggregate content was used, the compressive strength decreased due to a decrease in packing density, leading to greater risk of void space in the concrete matrix.

The same trend was observed for the 7-d surface resistivity, where the greatest electrical resistivity was obtained in the mixtures with near-to-maximum packing density (Figure 4.3b). Generally, the higher electrical resistivity corresponds to lower porosity. In the range of selected aggregate ratios, a lower percentage of sand is preferable to achieve satisfactory properties of concrete in both fresh and hardened states.

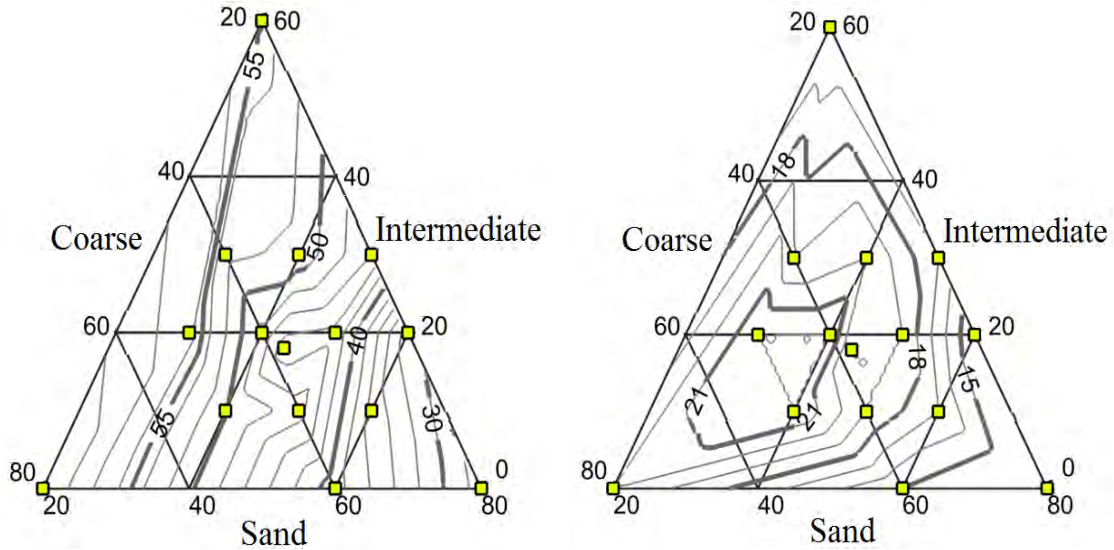

(a) 7-d compressive strength (b) 7-d electrical resistivity

Figure 4.3. Ternary diagrams of 7-d compressive strength and 7-d electrical resistivity of non-air-entrained RCC mixtures

The 28-d compressive strength and 14-d electrical resistivity ternary diagrams are depicted in Figure 4.4. All the tested compressive strengths observed were greater than the minimum value of 3500 psi (24.1 MPa) required for RCC pavement construction. The highest strength values were obtained in regions where the selected aggregate combinations are near the highest packing density of aggregates. The same trend was observed for the 14-d surface resistivity. Therefore, in the range of aggregates selected, lower sand content results in optimum hardened properties. This is near an aggregate combination with 40% coarse aggregate, 20% intermediate aggregate (or pea gravel), and 40% sand, by mass.

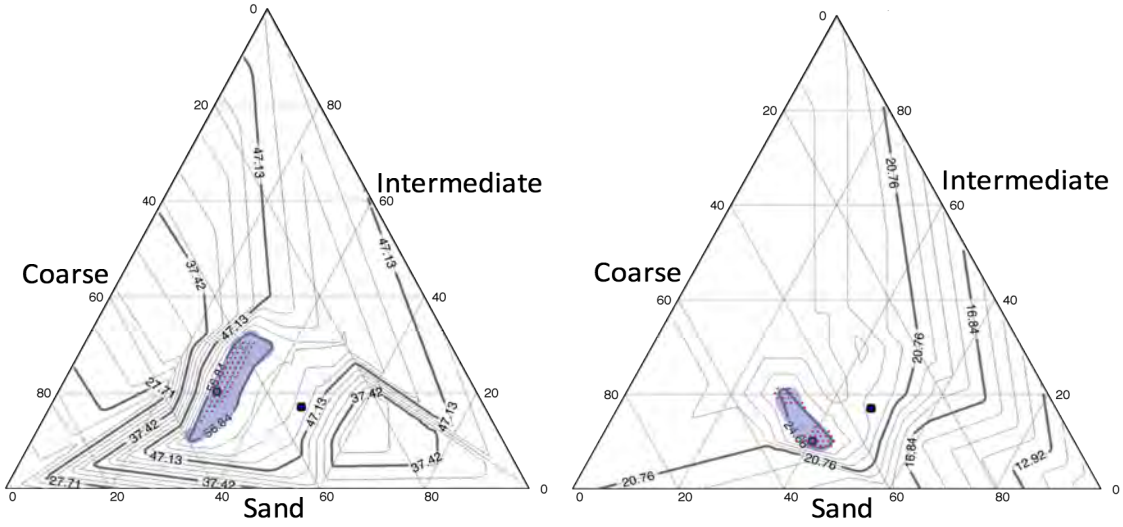

(a) 28-d compressive strength (b) 14-d electrical resistivity

Figure 4.4. Ternary diagrams of 28-d compressive strength and 14-d electrical resistivity of non-air-entrained RCC mixtures

4.2. Task 3 – Optimization of air-entrained RCC mixtures

4.2.1. Mixture proportions for air-entrained RCC mixtures

The optimized aggregate combination with 40% coarse aggregate, 20% intermediate aggregate, and 40% sand was air-entrained for the durability evaluation. The cementitious material content was adjusted to investigate the effect of binder level on RCC performance. The

mixtures were prepared with relatively low binder content of 430 (255 kg/m^3), medium content of 510 (303 kg/m^3), and high binder content of 580 lb/yd^3 (344 kg/m^3). A FAC was used at a substitution rate of 20% of the binder, by mass, except for mixtures with high binder content where a 40% replacement rate was used.

The dosage rates of the AEA varied from a medium dosage of 8 oz/yd^3 (309 ml/m^3), a high dosage of 16 oz/yd^3 (619 ml/m^3), and a very high dosage of 32 oz/yd^3 (1238 ml/m^3), by volume of concrete. The water-to-solid ratios (w/solid) of 5.5%, 5.6%, and 5.8% were used to adjust the low, medium, and high workability levels, respectively. The w/cm ranged from 0.4 to 0.42 as a result of change in workability. The Vebe time was used to evaluate the workability of the RCC.

A total of 11 air-entrained RCC mixtures with the following test parameters that are summarized in Table 4.4 were investigated:

(1) AEA dosage: medium (AM), high (AH), and very high (AV);

(2) Workability level: Vebe Time 90 - 60 s (WL), 60 - 30 s, and 30 - 15 s (WH);

(3) Binder volume: low (BL) and high (BH);

(4) Mixer type: Omni mixer (MO), drum mixer, and Eirich high shear rate mixer (MH);

(5) Compaction method: vibrating hammer (CH), Vebe vibrating table (CV), and ICT.

Table 4.5 shows the mixture proportioning of RCC mixtures with different AEA dosages and binder contents.

Table 4.4. Experimental matrix for RCC mixtures

Mix #	Binder volume			Workability level (VEBE TIME)			Mixer type			Compaction technique			AEA dosage		
	Low (430 lb/yd^3)	Medium (510 lb/yd^3)	High (580 lb/yd^3)	Low (60-90 s)	Medium (30-60 s)	High (15-30 s)	Omni	Drum	Eirich	Vibrating hammer	Vebe vibrating table	ICT	Medium (8 oz/yd^3)	High (16 oz/yd^3)	Very high (32 oz/yd^3)
AEA dosage level															
AM		x			x			x				x	x		
AH		x			x			x				x		x	
AV		x			x			x				x			x
Binder volume															
BL	x				x			x				x		x	
BH			x		x			x				x		x	
Workability level															
WL		x		x				x				x		x	
WH		x				x		x				x		x	
Mixer type															
MO		x			x		x					x		x	
MH		x			x				x			x		x	
Compaction technique															
CH		x			x			x		x				x	
CV		x			x			x			x			x	

Table 4.5. Mixture proportions of RCC mixtures with different AEA dosages and binder contents

Mix #	Mixture proportions (lb/yd^3)						Mixture parameter		
	Sand	Pea gravel	Coarse aggregate	Cementitious materials	Water	AEA (oz/yd^3)	w/cm	w/solid	Vebe time (s)
AM	1300	628	1327	510	227	8	0.40	5.5%	30 - 60 s
AH	1300	628	1327	510	227	16	0.40	5.5%	30 - 60 s
AV	1300	628	1327	510	227	32	0.40	5.5%	30 - 60 s
BL	1300	628	1327	430	172	16	0.40	5.5%	30 - 60 s
BH	1300	628	1327	580	232	16	0.40	5.5%	30 - 60 s

4.2.2. Mixture proportions for reference RCC mixtures

In order to compare the durability characteristics of air-entrained RCC developed in this research project, three additional reference mixtures were selected. The mixtures included the non-air-entrained mixture used in a field implementation of RCC in 2013 for the construction of Route 160 (RF), a reference RCC made without air entrainment (RN), and a mixture made with 44 oz/yd^3 (1707 ml/m^3) AEA (RA) that was laboratory tested by the authors in a previous project (Khayat and Liber, 2014). The mixture proportioning of the RCC mixture used in the field implementation was developed by the contractor and is not available. The mixture proportions of the RN and RA mixtures are summarized in Table 4.6. The mixtures had w/cm of 0.39 and a Vebe time of 30 s, which are similar to the RCC mixtures investigated in this project.

Table 4.6. Mixture proportions of the two reference mixtures of RN and RA

Mix #	Mixture proportions (lb/yd^3)							Mixture parameter		
	Sand	Crushed stone (1 in.)	Crushed stone (2 in.)	Fines (No. 200)	Cement	Water	AEA (oz/yd^3)	w/c	w/solid	Vebe time (s)
RN	1584	1155	561	1%	495	251	0	0.39	6.6%	30
RA	1534	1156	543	1%	590	249	44	0.33	6.6%	30

4.2.3. Compressive strength and surface resistivity

The compressive strength and surface resistivity at 7 to 28 days of the air-entrained RCC mixtures are summarized in Table 4.7. For the AH, AM, and AV mixtures, the increase in AEA dosage from 8 to 32 oz/yd^3 (309 to 1238 ml/m^3), by volume of concrete, slightly decreased the 28-d compressive strength.

The binder content had a significant effect on mechanical properties. The higher the binder content, the greater the compressive strength was. For example, the BL mixture made with a low binder content of 430 lb/yd^3 (255 kg/m^3) had a 28-d compressive strength of 5220 psi

(36 MPa); this value was 8400 psi (57.8 MPa) with the higher binder content of 580 lb/yd^3 (344 kg/m^3) which corresponds to an increase of 61%.

Compared to the WL mixture, the use of high workability level (Vebe time of 15 - 30 s) decreased the 7 and 28 d compressive strengths of the WH mixture by 2320 to 1740 psi (16 and 12 MPa), respectively. Such values were 41% and 18%, respectively, lower than those of the mixture with low workability level (Vebe time of 60 - 90 s). This might be due to greater air content in the mixture with high workability. The surface resistivity was also reduced by 10% to 42%, depending on curing age.

Table 4.7. Compressive and surface resistivity of air-entrained RCC mixtures

Mix #	Compressive strength, psi (MPa)		Surface resistivity (kΩ.cm)			
	7 d	28 d	7 d	14 d	21 d	28 d
AH	5210 (35.9)	7800 (53.5)	24	26	31	34
AM	5550 (38.3)	7800 (53.8)	25	27	34	35
AV	5730 (39.5)	7400 (51.0)	25	28	32	36
BL	3870 (26.7)	5220 (36.0)	19	25	26	28
BH	4840 (33.4)	8400 (57.9)	22	24	32	33
WL	5610 (38.7)	7990 (55.1)	22	24	31	34
WH	3190 (22.0)	6540 (45.1)	16	22	22	24
MO	5670 (39.1)	8290 (57.2)	24	29	29	33
MH	5240 (36.1)	7900 (54.5)	23	28	29	32
CV	3870 (26.7)	6540 (45.1)	18	22	23	29
CH	5410 (37.3)	7610 (52.5)	23	26	30	32

The mixer type had limited effect on compressive strength and surface resistivity of the RCC mixtures. The two RCC mixtures prepared using Omni and Eirich high shear mixer showed 28-d compressive strength and 28-d surface resistivity of 7250 psi (55 MPa) and (12.6 kΩ.in.) 32 kΩ.cm, respectively. However, the compaction technique exerted a great effect on the corresponding results. The mixture that was vibrated using a vibrating hammer (CH) displayed 7 and 28 d compressive strengths of 5410 (26.7 MPa) and 7610 psi (52.5 MPa), respectively,

which were 41% and 16% greater than those of the CV mixture compacted using a Vebe vibrating table. Besides, its surface resistivity values at different ages were 18% - 30% greater, indicating denser structure. Overall, the 28-d compressive strengths of all the tested mixtures exceeded 6540 psi (45 MPa). This meets the strength requirement of RCC for pavement construction. Besides, the values of surface resistivity of all the RCC mixtures ranged from 9.4 to 14.2 kΩ.in. (24 to 36 kΩ.cm), which are classified as moderate and/or low penetrability indexes.

4.2.4. Air-void system of air-entrained RCC mixtures

Using the Mechanical Rock Fragmentation Lab at Missouri S&T, extra specimens were cut with a rock saw to test the air-void system of those mixtures. The results of the air-void system, including spacing factor, air content, and specific volumes for < 0.02 in. (< 0.5 mm) and < 0.04 in. (< 1.0 mm) air voids, of air-entrained RCC are summarized in Table 4.8. Specific volume of RCC less than 635 in.$^{-1}$ (25 mm^{-1}) means good air-void system.

Table 4.8. Air-void system results for air-entrained RCC

Mix #	Spacing factor (μm)			Air content (%)			Specific volume (mm^2/mm^3)					
	1	2	Ave.	1	2	Ave.	< 0.5 mm	< 0.5 mm	Ave.	< 1.0 mm	< 1.0 mm	Ave.
AH	186	152	169	4.9	7.1	6.0	25.7	19.8	22.8	16.1	13.7	14.9
AM	251	196	224	4.8	5.2	5.0	16.7	18.6	17.7	13.2	14.6	13.9
AV	257	172	215	7.5	6.6	7.1	18.3	24.0	21.2	9.2	19.0	14.1
BL	173	130	152	7.2	6.5	6.9	19.2	31.1	25.2	13.6	12.8	13.2
BH	137	210	174	7.4	4.4	5.9	21.2	21.5	21.4	15.3	16.0	15.7
WL	95	176	136	4.4	7.4	5.9	41.2	17.5	29.4	30.6	12.1	21.4
WH	63	73	68	16.4	9.6	13.0	23.0	28.0	25.5	15.8	21.6	18.7
MO	106	131	119	4.3	7.5	5.9	33.3	26.6	30.0	25.7	20.0	22.9
MH	152	126	139	NA	NA	NA	NA	NA	NA	NA	NA	NA
CH	158	157	158	5.7	4.1	4.9	23.1	29.6	26.4	29.6	23.0	26.3

The spacing factors of all tested samples were below 0.009 in. (230 μm) and the air content was below 7%, suggesting acceptable results. The specific volumes of pores less than 0.02 and 0.04 in. (0.5 and 1.0 mm) were in the ranges of 457 - 762 $in.^{-1}$ (18 - 30 mm^{-1}) and 330 - 660 $in.^{-1}$ (13 - 26 mm^{-1}), respectively. It should be noted that at high workability level, the spacing factor and air void of the WH mixture were 0.009 in. (68 μm) and 13%, respectively, which were greatly different from the values of other mixtures of 0.006 - 0.009 in. (140 - 220 μm) and 5% - 7%, respectively. Due to the very low spacing factor, high air content, and specific volume, the WH mixture was retested to verify results. The high air void agreed well with the low compressive strength of RCC. It was found that the hardened properties and air-void system of the RCC mixtures were improved, except the high workability one.

4.2.5. Durability of RCC mixtures

(1) Freeze-thaw durability

The AH, WH, BL, and BH mixtures developed from this research work were selected for durability testing. Table 4.9 summarizes the mechanical properties of the selected five RCC mixtures. The 28-d compressive strengths are in the range of 7160 to 9160 psi (49.4 to 63.1 MPa). All tested concrete mixtures meet the strength requirement of RCC for pavement construction. The splitting tensile strength ranged from 440 to 650 psi (3.0 to 4.5 MPa). The measured values of modulus of elasticity in various RCC mixtures were greater than 8220 ksi (56.7 GPa), which are higher than the values estimated by ACI or AASHTO code for normal concrete. The higher modulus of elasticity is possibly due to the highly compacted solid structure of RCC, compared to conventional concrete.

Table 4.9 also summarizes the mechanical properties of the three reference mixtures. The splitting tensile strengths of the three mixtures were comparable to those of the four developed

RCC mixtures, whereas the values for the modulus of elasticity and compressive strength were lower. The RF cylindrical specimens measuring 6 × 12 in. (152 × 305 mm) showed 28-d compressive strength of 4310 psi (29.8 MPa), corresponding to an equivalent value of 4590 psi (31.7 MPa) for 4 × 8 in. (102 × 203 mm) specimens given a correction coefficient of 0.98 (Hake 2004). Despite the application of the correction factor for different specimen sizes, the compressive strength of the RF mixtures is considerably lower than the strength values for RCC mixtures tested using 4 × 8 in. (102 × 203 mm) cylindrical specimens. This might be due to different mixture designs between the RF mixture (field-tested) and the other mixtures developed by the research team in the laboratory.

Table 4.9. Mechanical properties of selected air-entrained RCC mixtures for durability testing

Mix #	Compressive strength (psi, MPa)		Splitting tensile strength (psi, MPa)	Modulus of elasticity (ksi, GPa)
	7 d	28 d		
AH	6200 (42.7)	7550 (52.1)	440 (3.0)	9430 (65.0)
WH	5740 (40.0)	7160 (49.4)	460 (3.2)	9590 (66.1)
BL	6890 (47.5)	8100 (55.8)	580 (4.0)	8720 (60.1)
BH	7230 (49.8)	9160 (63.1)	520 (3.6)	8220 (56.7)
RF *	3570 (24.6)	4310 (29.8)	420 (2.9)	4170 (28.9)
RF eq. strength**	3800 (26.2)	4590 (31.7)		
RN***	6250 (40.1)	6770 (46.7)	400 (2.8)	5510 (37.9)
RA***	6140 (42.3)	6370 (43.9)	440 (3.1)	5300 (36.5)

Note: * 6 × 12 in. (152 × 305 mm) cylinders consolidated by vibrating hammer for compressive strength testing;
** equivalent compressive strength of the RF specimens measuring 4 × 8 in. (102 × 203 mm) cylinders with a correction factor of 0.94;
*** 4 × 8 in. (102 × 203 mm) cylinders consolidated by vibrating hammer for compressive strength testing.

Figure 4.5 shows the specimens after 123 freeze-thaw cycles. The testing was stopped after 123 cycles because of obvious cracks that occurred in some specimens.

Figure 4.5. RCC specimens after 123 freeze-thaw cycles

Table 4.10 summarizes the mass loss of investigated RCC specimens subjected to 0, 36, 72, and 123 freeze-thaw cycles according to ASTM C 666, Procedure A. The mass loss increased with increasing cycles. After 123 cycles, the mass loss values of the four mixtures ranged from 1.8% to 3.1%.

Table 4.10. Mass loss of selected mixtures after certain freeze-thaw cycles

Mix #	Mass loss after certain cycles (%)			
	0	36	72	123
AH	0.00	0.10	0.85	2.13
BL	0.00	0.07	0.66	2.14
BH	0.00	0.07	1.57	3.12
WH	0.00	0.06	0.32	1.76

For the cast in field mixture (RF), all the specimens failed before 60 freeze-thaw cycles. Cracks even appeared in some specimens after 30 cycles, as shown in Fig. 4.6.

Figure 4.6. RCC specimens (RF mixture) cast in field after 30 freeze-thaw cycles (Khayat and Libre, 2014)

Figure 4.7 compares the durability factors of the four investigated RCC mixtures and the RF mixture took from the field. The durability factor corresponds to the square of the ratio of the dynamic modulus of elasticity of the concrete at N number of cycles to that at 0 cycle. Values of durability factor greater than 80% after 300 freeze-thaw cycles reflect adequate frost durability. The cast field mixture showed a low durability factor of 63% after 36 cycles and was damaged after that. For the four selected mixtures from this research, all the specimens demonstrated better frost resistance. After 72 cycles, the four RCC mixtures exhibited durability factors over 70%. This is because the specimens were deteriorated under continuous freezing and thawing damage. At 123 freeze-thaw cycles, the durability factor of the AH mixture was 54.4% and the other three RCC mixtures of BL, BH, and WH showed durability factors around 70%. The lower durability factor was attributed to poor air-void system associated with high air entrainment.

(2) Deicing salt-scaling resistance

Visual observations were used for rating the surface of concrete after every five freeze-thaw cycles. In addition, the scaling residues were collected and weighed to quantitatively evaluate the degree of surface deterioration. The visual ratings of the concrete surface before testing and after 50 cycles of freeze-thaw are given in Figure 4.8. It is obvious that the entrained air in RCC mixtures greatly improved the salt-scaling resistance. The reference RN mixture without any air entrainment exhibited the worst surface quality. In addition, the mixture with high binder content (BH) showed better surface quality than that of the one made with low binder content (BL).

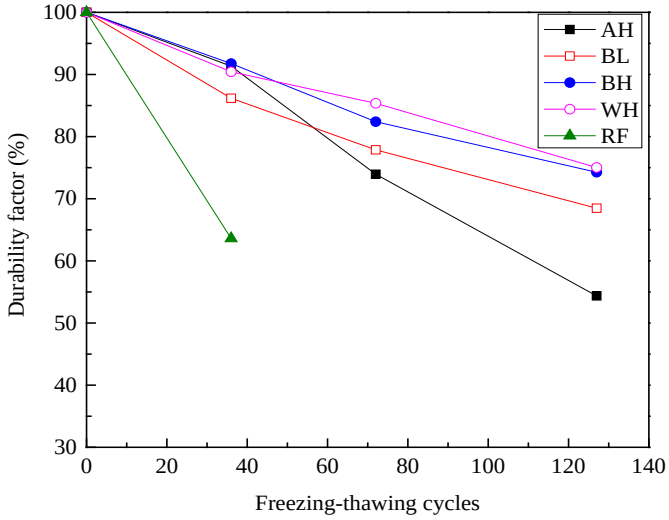

Figure 4.7. Durability factor of investigated RCC mixtures

Figure 4.9 presents the cumulative mass loss of the RCC mixtures during salt scaling testing after 50 freeze-thaw cycles. The scaled-off mass collected from the reference mixture FN (the non-air entrained mixture) was noticeably higher than other mixtures, especially after 30 cycles, which was 10.6 oz/yd^2 (360 g/m^2). This value increased rapidly with the increase of freeze-thaw cycles. At approximately 35 cycles, the cumulative loss was over 17.7 oz/yd^2 (600 g/m^2), which did not meet the threshold value as specified in the standard.

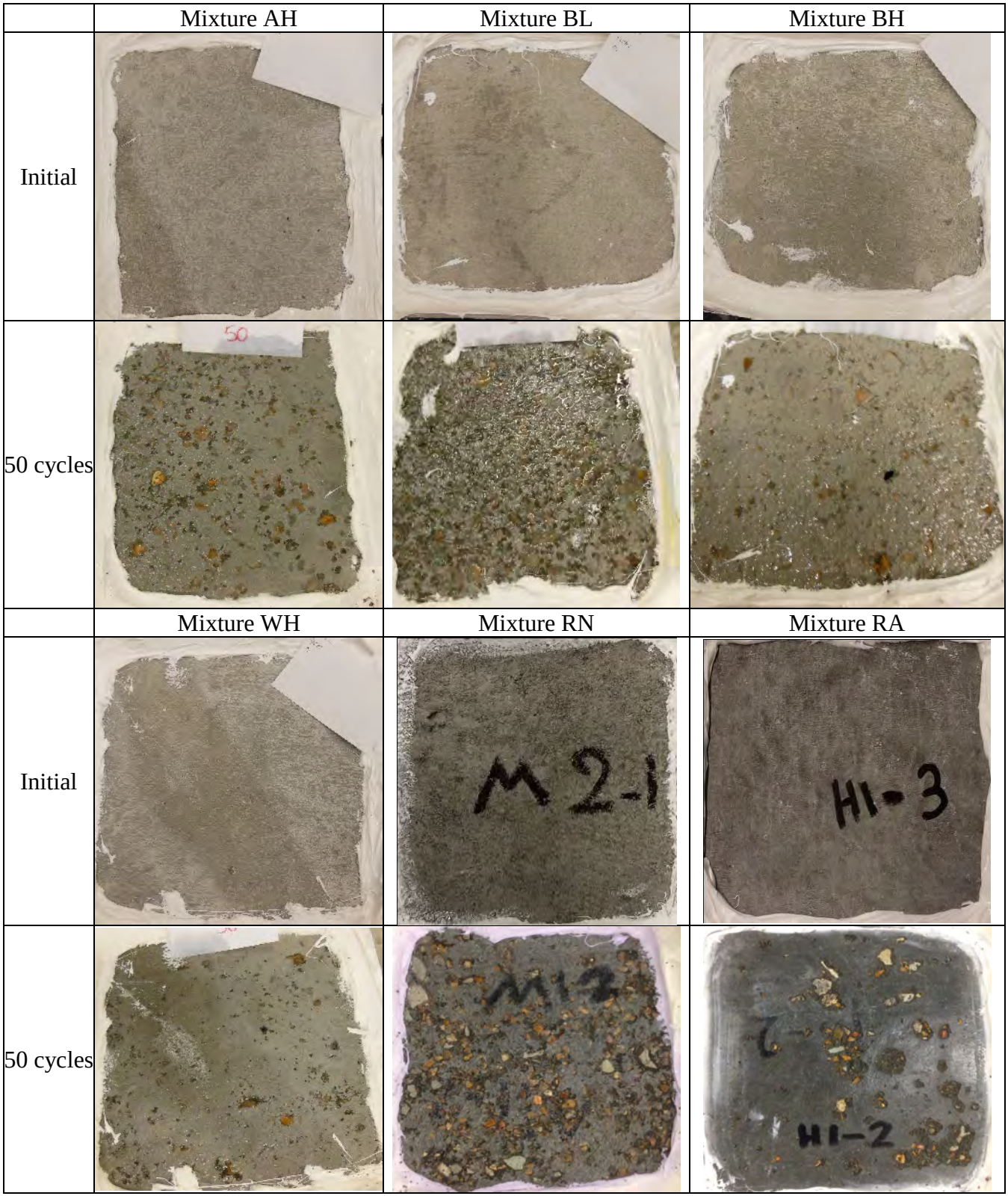

Figure 4.8. Surfaces of RCC specimens before and after 50 freeze-thaw cycles

The masses of scaling residues for all other air-entrained mixtures were found to vary between 1.8 and 12.1 oz/yd^2 (60 and 410 g/m^2) after 50 cycles. For all the air-entrained RCC mixtures, the average mass losses after 50 cycles were lower than 11.8 oz/yd^2 (400 g/m^2), which meets the limit of 29.5 oz/yd^2 (1000 g/m^2) as stated by PCA-2004 (2004). This indicates that the air entrainment significantly improves the durability of RCC mixtures.

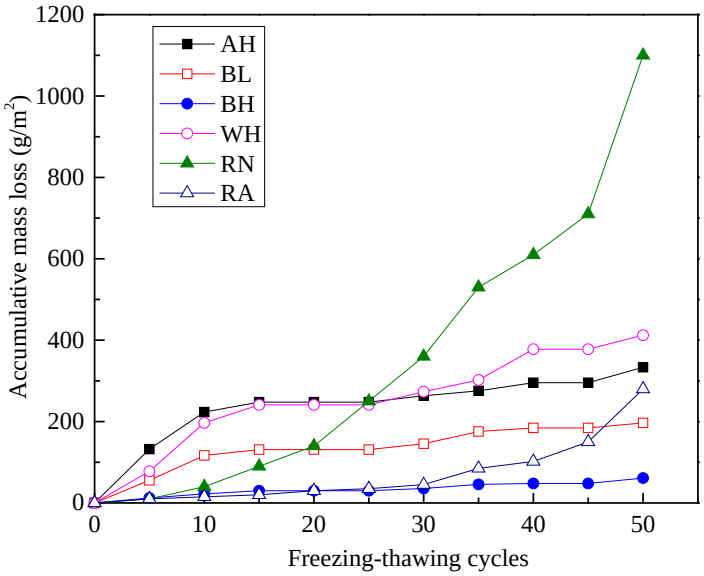

Figure 4.9. Cumulative mass loss of the RCC mixtures during salt scaling testing

The visual ratings of RCC surfaces after 50 freeze-thaw cycles are given in Table 4.11. This table also summarizes the results of permeable voids and water absorption test. Water absorption is mainly influenced by the interconnected capillary porosity in the paste. All the four developed mixtures exhibited comparable permeable voids and water absorption of approximately 7% and 3%, respectively, which were lower than those of the reference mixture. The low water absorption values of the developed RCC mixtures indicate good concrete in accordance with CEB-FIP (1989). The BH, WH, and RA mixtures showed the lowest level of

visual rating of one, which means very slight scaling. The AN mixture without air entrainment showed the highest visual rating of 4.

Table 4.11. Visual rating, permeable void, and water absorption of the five RCC mixtures

Mix #	Permeable void	Water absorption	Deicing salt scaling
	%	%	Visual rating after 50 cycles
AH	7.44	3.26	2.0
BL	6.93	3.07	3.0
BH	7.55	3.39	1.0
WH	7.32	3.19	1.0
RN	9.98	3.60	4.0
RA	9.56	4.00	1.0

5. Task 4 - RECOMMENDATION OF RCC MIXTURE PROPORTIONING FOR FIELD IMPLEMENTATION

The research can contribute to the development and implementation of new mixture design methodology and quality control tools for the design and construction of concrete pavement using RCC. The use of RCC can accelerate concrete pavement construction and improve mechanical and long-term performance, leading to reduced life-cycle cost of the transportation infrastructure. Meanwhile, the outcomes of the research can provide guidelines for the selection of concrete constituent materials, mixture optimization methodology, and performance-based specifications, and construction guidelines of RCC pavement. Based on the results obtained from this study, the following recommendations can be made for RCC field implementation.

5.1. Mixture proportioning

Selection of optimal combination of aggregate as the solid skeleton for RCC materials is the first essential step for RCC mixture proportioning. Aggregate combinations of crushed and rounded aggregates with various combinations of fine, intermediate, and coarse aggregate contents can be used to prepare RCC. The PSD can be optimized by using empirical PSD optimization software and grading models. Statistical mixture design method can be applied to select the optimum aggregate combination to achieve the maximum possible packing density. Generally, smooth and rounded combinations exhibit higher packing density compared to the crushed and rough aggregate combinations. However, crushed aggregates are preferred because of the interlocking friction among the particles, thus reducing the risk of aggregate segregation. After determining the skeleton of aggregate for RCC mixture, the workability and mechanical

properties of RCC should be checked. High content of coarse aggregate can increase the voids between the aggregate skeleton and eventually decreased strength, while increasing the sand and intermediate aggregate contents can increase the risk of segregation of the RCC mixture. Therefore, the workability, density, strength, and even durability characteristics need to be considered for the selection of aggregate blend and binder contents.

Incorporation of air-entraining agent in RCC can affect the porosity, compressive strength, and durability characteristics. The air content and the stability and uniformity of air bubbles are greatly affected by several parameters, such as binder content, mixing procedure, workability level, and compaction techniques. Results from this research indicated that RCC mixtures with spacing factors below 0.009 in. (230 μm) and air content below 7% suggest an acceptable air-void system. High workability is harmful to the stability of air bubbles because it can make them easily move.

5.2. Properties of RCC mixtures

Given the binder content, the fresh and hardened properties of RCC mixtures are greatly affected by the aggregate combination. Increasing the sand content in RCC mixtures can increase the Vebe time (reduced workability), the segregation risk, as well as the reduction in strength of the RCC mixture. However, an increase in coarse aggregate can reduce the strength and electrical resistivity of the RCC mixture due to a decrease in the packing density of the system. Therefore, high packing density of the aggregate skeleton, proper workability, and high strength of RCC mixture should be secured to design optimal RCC mixtures. Satisfactory RCC mixtures should be designed to have packing density around 0.8, Vebe time in the range of 30 - 60s, and 28-d compressive strength over 3630 psi (25 MPa), and moderate and/or low value of surface resistivity ranged from 9.4 to 14.2 kΩ.in. (24 to 36 kΩ.cm).

Binder content, workability level, and compaction technique greatly affect the mechanical properties and air-void system of the RCC mixtures, while AEA dosage and mixer type have limited effect on the mechanical properties. The higher the binder content is, the greater the compressive strength and electrical resistivity are. RCC with a binder content of 430 lb/yd^3 (255 kg/m^3) is shown to have satisfactory mechanical properties and durability. Use of 20% to 40% fly ash can be added in binary RCC to reduce cement content and enhance strength and durability characteristics. High workability level can decrease compressive strength and surface resistivity. Compaction techniques play a significant role in influencing the strength and durability of RCC. Sufficient compaction is needed to secure frost and salt-scaling resistance of RCC in cold regions. Besides, the introduction of AEA in RCC mixtures significantly improved the frost and salt-scaling resistance. The recommended AEA dosages RCC with w/cm ratio of 0.4 can be in the range of 16 to 44 oz/yd^3 (619 to 1707 ml/m^3), by volume of concrete.

6. CONCLUSIONS

6.1. Conclusions

The research presented in this project was developed to design and formulate a new class of high-performance RCC that can exhibit adequate workability and frost durability for the use in accelerated pavement applications. Several parameters contributing to the formulation of such concrete mixtures were investigated, including aggregate proportion and air void system. Fresh and hardened properties of RCC made with different aggregate types, shapes, and proportions from various quarries covering a wide range of aggregates available in Missouri were investigated. The optimized RCC mixture with high packing density of aggregate combination, suitable workability, and mechanical properties were then used to introduce air entrainment. Effect of several parameters, including AEA dosage, binder content, workability level, mixing type, and energy on mechanical properties and durability were investigated.

6.1.1. Optimization of aggregate skeleton

The packing densities of selected aggregates with different nominal maximum sizes (fine, intermediate, and coarse) and shapes (crushed and rounded) were then determined using the ICT. Aggregate combinations having different proportions of fine, intermediate, and coarse aggregates were evaluated. The possible maximum packing density values that can be obtained for different aggregate combinations were determined. Based on the above results, the following conclusions can be drawn:

- The packing density of aggregate can vary with the nominal maximum size, shape, surface texture, and angularity of the aggregate.
- The packing densities of the investigated fine, intermediate, and coarse aggregates vary in the range of 0.58 - 0.72, 0.60 - 0.68, and 0.59 - 0.61, respectively.

- Given different aggregate combinations and proportions, the packing density (Φ) of the investigated ternary aggregate combinations varied from 0.63 to 0.82. The optimal aggregate combination was found to be 40% sand, 20% intermediate aggregate, and 40% coarse aggregate that had a high packing density greater than 0.80.
- Regardless of the aggregate type, the packing density increased with the increase in fine-to-total aggregate ratio up to a certain threshold value, beyond which the maximum packing density decreased with further increase in fine aggregate.
- The void ratio (1-Φ) corresponds to the minimum volume of paste needed to fill the voids between aggregate particles. The void ratio of the selected aggregate combinations varied from 0.37 to 0.28. This indicates that the minimum paste content can be reduced by 32% by optimizing the aggregate combinations to reduce the void ration, hence resulting in more cost-effective RCC mixtures.

6.1.2. Performance evaluation of non-air-entrained RCC mixtures

The Vebe time, segregation index, compressive strength, and bulk electrical resistivity of 17 RCC mixtures made with different aggregate combinations and no air entrainment were investigated. Based on the test results, the following conclusions can be drawn:

- Increasing the sand content was shown to increase the Vebe time (reduced workability). The risk of segregation also increased with the increase in sand and intermediate aggregate contents.
- All compressive strength values were greater than the minimum value of 3500 psi (24.1 MPa) required for RCC pavement construction. The highest strength and surface resistivity values were obtained for aggregate combinations corresponding to the highest packing density.

- RCC mixture made with the optimized aggregate combination of 40% coarse aggregate, 20% intermediate aggregate (or pea gravel), and 40% sand exhibited the best workability, compressive strength, and electrical resistivity performance.

6.1.3. Optimization of air-entrained RCC mixtures

The optimized RCC mixture with 40% coarse aggregate, 20% intermediate aggregate (or pea gravel), and 40% sand was used to prepare air-entrained mixtures. The effect of different parameters, including AEA dosage, binder content, workability level, mixer type, and compaction technique on mechanical properties and durability were investigated. The air-void system, including the air content in the hardened concrete, spacing factor, and specific volume were determined. In total, 11 air-entrained RCC mixtures were investigated, Based on the findings from this phase, the following conclusions can be summarized:

- The 28-d compressive strength of RCC mixtures exceeded 5220 psi (36 MPa), which meets the strength requirement of RCC for pavement construction.
- The surface resistivity ranged from 9.4 to 14.2 kΩ.in. (24 to 36 kΩ.cm), which is classified as moderate and/or low penetrability.
- For a given binder content, the increase in AEA dosage from 8 to 32 oz/yd^3 (309 to 1238 ml/m^3) slightly decreased the 28-d compressive strength and electrical resistivity.
- The increase of the binder content resulted in greater compressive strength. For example, increasing the binder content from 430 lb/yd^3 (255 kg/m^3) to 580 lb/yd^3 (344 kg/m^3) led to 28-d compressive strength varying from 5220 psi (36 MPa) to 8340 psi (57.8 MPa), corresponding to 61% increment.
- The proportioning of RCC with high workability level (Vebe time of 15 - 30 s) decreased the 7- and 28-d compressive strengths by 41% and 18%, respectively, compared to RCC

with low workability level (Vebe time of 60 - 90 s). The surface resistivity of the former mixture was also reduced by 10% to 42%, depending on curing age.

- The mixer type used to prepare the RCC mixtures had limited effect on compressive strength and surface resistivity. The two RCC mixtures prepared using the Omni and Eirich high shear mixer had similar 28-d compressive strength and 28-d surface resistivity results of 7250 psi (55 MPa) and 12.6 kΩ.in. (32 kΩ.cm), respectively.
- The compaction technique used to consolidate RCC test specimens had a significant effect on mechanical properties. Specimens vibrated using a vibrating hammer had 7- and 28-d compressive strength values of 5410 psi (26.7 MPa) and 7610 psi (52.5 MPa), respectively, which are 41% and 16% greater than those of the mixture compacted using the Vebe vibrating table. The surface resistivity values of the former compaction technique were 18% - 30% greater at different ages, indicating denser structure.
- Proper spacing factor below 0.009 in. (230 μm) was achieved for the developed air-entrained RCC mixtures. The hardened properties and air-void system of the RCC mixtures having lower workability were better than RCC mixtures with lower Vebe time values. The 28-d compressive strength and electrical resistivity of the RCC with the higher Vebe time were 18% and 29%, respectively, greater than the same concrete that had a lower Vebe time. This spread in hardened properties is associated with the 55% higher air content of the more workable air-entrained RCC (hardened air content of 13% compared to 5% to 7%).

6.1.4. Durability of optimized air-entrained RCC mixtures

Four air-entrained RCC mixtures developed in this research project were selected for frost durability evaluation. The freeze-thaw and deicing salt-scaling results were compared to the

durability characteristics of a reference air-entrained and non-air-entrained RCC mixtures developed during a laboratory investigation carried out by the authors in 2013 and an experimental RCC pavement construction in 2013 in Doniphan, MO, involving a non-air-entrained RCC. Based on the test results, the following main findings can be established:

- The non-air-entrained RCC mixture used for the field construction in 2013 showed a low durability factor of 63% after only 36 freeze-thaw cycles; the test specimens cracked soon after.
- The four optimized air-entrained RCC mixtures had durability factors of approximately 70% after 123 freeze-thaw cycles. However, the specimens failed soon after, and their frost durability levels can be considered marginal despite of the proper air-void system.
- The de-icing salt scaling mass loss of the reference mixture without any air-entrainment was noticeably higher than other mixtures. The cumulative loss after approximate 35 cycles was over 17.7 oz/yd^2 (600 g/m^2). On the other hand, the air-entrained RCC mixtures exhibited high salt-scaling resistance with average mass loss lower than 11.8 oz/yd^2 (400 g/m^2) after 50 cycles, which is considerably lower than the limit of 29.5 oz/yd^2 (1000 g/m^2).

6.2. Future work

Test results presented and discussed in this report confirm the importance of optimizing the PSD of the aggregate skeleton in proportioning RCC as well as the possibility to properly air-entrain RCC. The following research is required for further development of RCC for rapid pavement construction:

- The degree of compaction for RCC specimens can vary depending on the consolidation effort. A comparison should be carried out between mechanical properties of RCC samples prepared using the standard vibrating hammer technique and in-situ measurements of RCC compacted using a vibrating roller.
- The investigators will assist in the planning, field implementation, and monitoring of pilot projects in which optimized air-entrained RCC mixtures developed in this project will be employed. With regard to the experience of the previous experimental sites, such as the RCC project in Doniphan of 2013, it is proposed to cast sections of pavement on city streets and/or highways. A test section with an approximate length of at least 100 ft (30 m) is proposed to be cast with each pavement type. For each field site, several pavement panels will be placed using different optimized mixtures. The concrete will be instrumented to investigate variations of temperature, moisture, and deformation.
- It is required to investigate the long-term in-situ deformation characteristics of the pavement. Relative humidity sensors, vibrating wire strain gages (VWSGs), and thermocouples will be used to evaluate in-situ performance.
- Concrete samples will be taken at the batching plant to monitor fresh properties, mechanical properties, shrinkage, and durability characteristics. In addition, samples will be extracted from the pavement to investigate in-situ properties, including mechanical properties, bond strength between different lifts, and durability.
- Stress-strain behavior of the pavement sections will be evaluated using controlled load testing with truck loading and falling weight deflectometer (FWD). For this reason, it is required to install sensors at different depths at the wheel-path of the pavement lanes to monitor the deformations caused by certain amounts of loading.

REFERENCES

American Concrete Institute, ACI Concrete Terminology, American Concrete Institute, Farmington Hills, MI, http:// Terminology.concrete.org (accessed Jan. 14, 2008). 2010.

AASHTO T95. Standard Method of Test for Surface Resistivity Indication of Concrete's Ability to Resist Chloride Ion Penetration. 2014.

Angelakopoulos, H., Neocleous, K., Pilakoutas, K., Steel fiber reinforced roller-compacted concrete road, Int. Intersec., 2009, 6(1), 45-55.

ASTM C33 / C33M. Standard Specification for Concrete Aggregates. 2016.

ASTM C109/C109M. Standard Test Method for Compressive Strength of Hydraulic Cement Mortars (Using 2-in. or [50-mm] Cube Specimens). 2016.

ASTM C418. Standard Test Method for Abrasion Resistance of Concrete by Sandblasting, 2012.

ASTM C 457, Microscopic Determination of Air-Void Content and Parameters of the Air-Void System in Hardened Concrete, 2016.

ASTM C469/C469M-14 Standard Test Method for Static Modulus of Elasticity and Poisson's Ratio of Concrete in Compression. 2014.

ASTM C496/C496M. Standard Test Method for Splitting Tensile Strength of Cylindrical Concrete Specimens. 2017.

ASTM C642, Standard Test Method for Density, Absorption, and Voids in Hardened Concrete. 2013.

ASTM C666/C666M, Standard Test Method for Resistance of Concrete to Rapid Freezing and Thawing. 2003.

ASTM C672/C672M-12 Standard Test Method for Scaling Resistance of Concrete Surfaces Exposed to Deicing Chemicals, 2012.

ASTM C779. Standard Test Method for Abrasion Resistance of Horizontal Concrete Surfaces. 1974.

ASTM C 994. Standard Test Method for Abrasion Resistance of Concrete or Mortar Surfaces by the Rotating Cutter Method. 1999.

ASTM C1170, Standard Test Method for Determining Consistency and Density of Roller-Compacted Concrete Using a Vibrating Table. 2014.

ASTM C1176/C1176M. Standard Practice for Making Roller-Compacted Concrete in Cylinder Molds Using a Vibrating Table. 2013.

ASTM C1435 / C1435M. Standard Practice for Molding Roller-Compacted Concrete in Cylinder Molds Using a Vibrating Hammer. 2008.

Cetin A., Carrasquillo R.L., High-performance concrete: influence of coarse aggregates on mechanical properties. ACI Mater J 1998;95(3):252-261.

CEB-FIP. Diagnosis and assessment of concrete structures – state of art report. CEB Bull 1989;192:83-85.

Delatte, N., & Storey, C., Effects of density and mixture proportions on freeze-thaw durability of roller-compacted concrete pavement. Transportation Research Record: Journal of the Transportation Research Board, 1914, 2005, 45-52.

Ghafoori, N., Cai, Y., Laboratory-Made RCC containing Dry Bottom Ash: Part I - Mechanical Properties. Mater. J., 1998, 95(2), 121-130.

Hake, P.J., Comparison of compressive strengths using 4 × 8 vs. 6 × 12 cylinders for prestress concrete (No. RDT 04-005), 2004.

Hazaree, C., Ceylan, H., & Wang, K.. Influences of mixture composition on properties and freeze-thaw resistance of RCC. Constr. and Build. Mater. 2011, 25(1), 313-319.

Harrington, D., Abdo, F., Adaska, W., Hazaree, C.V., Ceylan, H., Bektas, F., Guide for roller-compacted concrete pavements. 2010.

Highways, Missouri,. and Transportation Commission, 2004. Missouri Standard Specifications for Highway Construction, 2004. Missouri Highways and Transportation Commission.

Kagaya, M., Suzuki, T., Kokubun, S. and Tokuda, H., A study of mix proportions and properties of steel fiber reinforced roller-compacted concrete for pavements, Tran. Proc. JSCE, 2001, 50 (669), 16.

Khayat, K.H. and Libre, N.A., Roller compacted concrete: field evaluation and mixture optimization (No. NUTC R363). Missouri University of Science and Technology. Center for Transportation Infrastructure and Safety. 2014.

Khayat, K.H., Mehdipour, I., Design and performance of crack-free environmentally friendly concrete "Crack-Free Eco-Crete," Report cmr17-007.

Khayat, K. H., Nicolas Ali Libre, Roller Compacted Concrete: Field Evaluation and Mixture Optimization. 2014.

Kreijger, P.C., The Skin of Concrete: Composition and Properties, Materials and Structures, Research and Testing (RILEM, Paris), 17 (100), July-Aug. 1984, pp. 275-283.

Liu, T. C., Performance of Roller Compacted Concrete – Corps of Engineers' Experience, ACI Special Publication SP-126, Durability of Concrete, Second International CANMET/ACI Conference, Vol. II, 1991, pp. 155-167.

Madhkhan, M., Azizkhani, R., Torki, M.E., Roller compacted concrete pavements reinforced with steel and polypropylene fibers, Struct. Eng. Mech., 2011, 40(2), pp. 149-165.

Madhkhan, M., Azizkhani, R., Torki, M.E., Effects of pozzolans together with steel and polypropylene fibers on mechanical properties of RCC pavements, J. Construct. Build. Mater., 2012, 26(1), pp. 102-112.

Madhkhan, M., Nowroozi, S., Torki, M.E., Flexural strength of roller compacted concrete pavements reinforced with glass-roved textiles. Structural Engineering and Mechanics, 2015, 55(1).

Mardani-Aghabaglou, A., Andiç-Çakir, Ö., Ramyar, K., Freeze–thaw resistance and transport properties of high-volume fly ash roller compacted concrete designed by maximum density method. Cem. Concr. Compos., 2013, 37, pp. 259-266.

Mehdipour, I., Characterization and performance of eco and crack-free high-performance concrete for sustainable infrastructure. 2017.

Nanni, A., Abrasion resistance of roller compacted concrete. ACI Materials Journal, 1989, 86(6), pp. 559-565.

Piarc Technical Committee on Concrete Roads, The Use of Roller Compacted Concrete for Roads. 1993.

Rollings, R.S., Design of Roller Compacted Concrete Pavements, Proceedings, Roller Compacted Concrete II (February 29-March 2, 1988, San Diego, CA, 1988, Edited by Kenneth D. Hansen and Leslie K. Guice), American Society of Civil Engineers (ASCE), New York, NY, USA, pp. 454-466.

PCA, RCC Newsletter, Vol. 10, No. 1, Fall, Portland Cement Association, Skokie, IL, USA, 4 pages, 1994.

Portland Cement Association (PCA), (2004). Cement Shortage Analysis. The Monitor Flash Report, May 13, Skokie:IL.

Piggott, R. W., Roller Compacted Concrete Pavements - A Study of Long Term Performance, RP366.01P, Portland Cement Association, Skokie, IL, USA, 62 pages, 1999.

Sun, Z.H., and Scherer, G.W., Effect of air voids on salt scaling and internal freezing. Cem. Concr. Res, 2010, 40(2), pp. 260-270.

Tayabgi, S.D. and Okamoto, P.A., Engineering Properties of Roller Compacted Concrete, Transportation Research Record 1136, 1987, Transportation Research Board, Washington, D.C..

Vahedifard, F., Nili, M., & Meehan, C. L. Assessing the effects of supplementary cementitious materials on the performance of low-cement roller compacted concrete pavement. Constr. and Build. Mater., 2010, 24(12), pp. 2528-2535.

Valenza, J.J., II, Vitousek, S., and Scherer, G.W. Expansion of hardened cement paste in saline solutions. Creep, shrinkage and durability of concrete and concrete structures, G. Pijaudier-Cabot, B. Gérard, and P. Acker, eds., Hermes, London, 2005, pp. 207-212.